From the Department of Clinical Science, Intervention and Technology (CLINTEC), Division of Orthopedics and Biotechnology
Karolinska Institutet, Stockholm, Sweden

ACHILLES TENDON LOADING AND DEFORMATION DURING REHABILITATION AND USE OF ANKLE FOOT ORTHOSES

Åsa Fröberg

Stockholm 2018

Cover illustration by Tommy Fröberg
All previously published papers were reproduced with permission from the publisher.
Published by Karolinska Institutet.
Printed by E-print AB 2018

ISBN 978-91-7831-090-6

Institutionen för klinisk vetenskap, intervention och teknik (CLINTEC), Enheten för ortopedi och bioteknologi

ACHILLES TENDON LOADING AND DEFORMATION DURING REHABILITATION AND USE OF ANKLE FOOT ORTHOSES

AKADEMISK AVHANDLING

som för avläggande av doktorsexamen vid Karolinska Institutet offentligen försvaras i föreläsningssal B64 Karolinska Universitetssjukhuset, Huddinge

Onsdagen den 20 juni 2018 klockan 09.00

av

Åsa Fröberg
Specialistläkare

Huvudhandledare:
Professor Toni Arndt
Gymnastik- och idrottshögskolan och
Karolinska Institutet
Institutionen för klinisk vetenskap,
intervention och teknik (CLINTEC)
Enheten för ortopedi och bioteknologi

Bihandledare:
Docent Tomas Movin
Karolinska Institutet
Institutionen för klinisk vetenskap,
intervention och teknik (CLINTEC)
Enheten för ortopedi och bioteknologi

Professor Birgitta Janerot Sjöberg
Karolinska Institutet
Institutionen för klinisk vetenskap,
intervention och teknik (CLINTEC)
Enheten för funktion och teknologi

Fakultetsopponent:
Professor Jon Karlsson
Göteborgs Universitet Sahlgrenska Akademin
Institutionen för kliniska vetenskaper
Avdelningen för ortopedi

Betygsnämnd:
Docent Wim Grooten
Karolinska Institutet
Institutionen för neurobiologi, vårdvetenskap
och samhälle
Sektionen för fysioterapi

Docent Pernilla Eliasson
Linköpings Universitet
Institutionen för klinisk och experimentell
medicin
Avdelningen för kirurgi, ortopedi och onkologi

Docent Christer Grönlund
Umeå Universitet
Institutionen för strålningsvetenskaper
Enheten för radiofysik

Nu Karl, Amanda och Nils är boken klar…

ABSTRACT

Achilles tendon rupture is a common injury which most often affects otherwise healthy individuals and which causes long periods of rehabilitation with absence from work and sport activities and frequently sequele with reduced calf muscle performance. The aim of this thesis is to improve understanding of how injury affects the function of the Achilles tendon, and to functionally evaluate different designs of ankle foot orthoses used during rehabilitation after an Achilles tendon rupture. A non-invasive ultrasound based method for estimating tissue motion is also adapted and evaluated for use on the Achilles tendon during motion.

In the first study of this thesis an adjustable ankle foot orthosis was investigated regarding its effect on force in the Achilles tendon and muscle activity in the lower leg during walking. Unexpectedly force in the Achilles tendon was found to be higher at certain ankle foot orthoses settings than for barefoot walking. These results raised the question if different designs of ankle foot orthoses affect the Achilles tendon in different ways. To pursue this question, a non-invasive method of studying Achilles tendon biomechanics was required. Advances in tissue displacement and strain estimation in echocardiography lead to the choice of ultrasound based speckle tracking. In the second study of this thesis a commercial ultrasound speckle tracking algorithm was evaluated for estimation of strain in tendon tissue in a series of in-vitro experiments. Results of this study showed high variability in measurement errors which lead to the decision to adapt and use an in-house developed speckle tracking algorithm instead. In the first part of study III, an in-house developed speckle tracking algorithm was adapted and evaluated for displacement estimation in tendons. Results showed a high correlation between estimated tendon displacement and reference values, but a constant underestimation of displacement. For the magnitude and velocity of displacement relevant during range of motion exercise and walking, low coefficients of variation were found. In the second part of study III the in-house developed speckle tracking algorithm was implemented on ultrasound images of uninjured and previously ruptured Achilles tendons during motion. Displacement in superficial and deep tendon layers was estimated and it was found that the non-uniform displacement pattern observed in uninjured tendons was disturbed following injury. Displacement in different parts of the tendons could be distinguished with statistical significance indicating that the speckle tracking algorithm was clinically applicable. In study IV, ultrasound speckle tracking, electromyography of the lower leg muscles and plantar pressure measurement were combined to investigate how the Achilles tendon is affected by the use of three different designs of ankle foot orthoses with varying degrees of dorsiflexion limitation. Results show that the degree of dorsiflexion limitation within an ankle foot orthosis seems to affect tendon displacement patterns and lower leg muscle activity to a greater extent than differences in ankle foot orthosis design.

In conclusion, ultrasound based speckle tracking for estimation of tendon motion is feasible and can be used to investigate alterations in Achilles tendon deformation patterns following injury and during use of different designs of ankle foot orthoses.

SAMMANFATTNING

Att slita av hälsenan är en vanlig skada som leder till lång rehabilitering med frånvaro från arbete och sportaktiviteter, och ofta kvarstående besvär med nedsatt funktion i vadmuskeln. Syftet med den här avhandlingen är att öka kunskapen om hur skador påverkar hälsenans funktion. Vidare undersöks hur några vanliga modeller av fotledsortoser som används i behandlingen av hälsenerupturer påverkar senan vid gång. En ultraljudsbaserad metod för att mäta rörelser i vävnader anpassas och utvärderas för användning på hälsenan.

I den första studien undersöktes en ortos med justerbar fotledsvinkel. Kraften i hälsenan och muskelaktiviteten i underbenet mättes vid olika fotledsvinklar och jämfördes med barfota gång. Oväntat nog var kraften i hälsenan högre när ortosen användes med vissa vinkelinställningar än vid barfota gång. Resultaten ledde till hypotesen att olika modeller av ortoser påverkar hälsenan på olika sätt. För att undersöka detta vidare behövdes en ny metod för att mäta mekanisk påverkan på hälsenan som fungerar utan att man behöver skära eller sticka i senan. Framsteg inom ultraljudsundersökningar på hjärtat med mätningar av rörelse och töjning i vävnaden ledde till valet av ultraljudsbaserad bildanalys, så kallad speckle tracking. I en serie experiment i den andra studien i den här avhandlingen utvärderades ett speckle tracking program utvecklat för analys av töjning i hjärtmuskel, för att se om det kunde användas även på senvävnad. Resultaten visade stor variation i mätfelet vilket gjorde metoden opålitlig. Istället anpassades ett speckle tracking program för analys av vävnadsrörelser som utvecklats inom forskargruppen och i del ett av den tredje studien i avhandlingen testades programmet på senvävnad i laboratorieexperiment. Det fanns ett tydligt samband med referensvärden men bildanalysprogrammet underskattade delvis rörelserna i senan. I del två av den tredje studien användes bildanalysprogrammet för att analysera rörelsemönstret i oskadade och tidigare skadade senor. De oskadade senorna hade ett asymmetriskt rörelsemönster med större rörlighet i djupa delar av senan än i ytliga delar, vilket tros vara viktigt för vadmuskelfunktionen. I tidigare skadade senor var rörelsemönstret homogent från ytligt till djupt. Bildanalysprogrammet kunde särskilja rörlighet i olika delar av senan med statistisk signifikans. I den fjärde studien undersöktes rörelsemönstret i hälsenan, aktiviteten i underbenets muskulatur och tryckfördelningen under fotsulan vid gång dels barfota och dels när tre olika modeller av ortoser användes. Ortoserna testades med olika vinkel i fotleden. Resultaten visade att fotledsvinkeln påverkade rörelsemönstret i hälsenan och aktiviteten i underbenets muskulatur mer än valet av ortosmodell.

Sammanfattningsvis visade avhandlingen att ultraljudbaserad speckle tracking kan användas för att analysera rörelser i senvävnad. Hälsenans rörelsemönster påverkas av tidigare skada i senan och kan även påverkas vid användning av ortoser genom att vinkeln i fotleden ändras.

LIST OF SCIENTIFIC PAPERS

I. Fröberg Å, Komi P, Masaki I, Movin T, Arndt A.
Force in the Achilles tendon during walking with ankle foot orthosis.
Am J Sports Med. 2009; 37: 1200-1207.

II. Fröberg Å, Mårtensson M, Larsson M, Janerot-Sjöberg B, D'Hooge J, Arndt A.
High variability in strain estimation errors when using a commercial ultrasound speckle tracking algorithm on tendon tissue.
Acta Radiol. 2016; 57: 1223-1229

III. Fröberg Å, Cissé A-S, Larsson M, Mårtensson M, Peolsson M, Movin T, Arndt A.
Altered patterns of displacement within the Achilles tendon following surgical repair.
Knee Surg Sports Traumatol Artrosc. 2017; 25: 1857-1865.

IV. Fröberg Å, Mårtensson M, Arndt A.
The effect of three commonly used designs of ankle foot orthoses on Achilles tendon biomechanics – tendon deformation, calf muscle activation and plantar pressure during walking.
Manuscript

CONTENTS

LIST OF ABBREVIATIONS

AFO	ankle foot orthoses
ANOVA	analysis of variance
AT	Achilles tendon
bf	barefoot
CI	confidence interval
df	dorsiflexion
disp	displacement
EMG	electromyography
gcm	gastrocnemius mediale
gcl	gastrocnemius laterale
GRF	ground reaction force
MVC	maximum voluntary contraction
Pa	Pascal, unit of pressure, 1 Pa = 1 N/m^2
PC	personal computer
pf	plantarflexion
PVA	polyvinyl alcohol
RMSE	root mean square error
ROI	region of interest
SD	standard deviation
sol	soleus
STA	speckle tracking algorithm
ta	tibalis anterior
wdg	wedge

1 BACKGROUND

1.1 INTRODUCTION

Acute rupture of the Achilles tendon most commonly occurs during sport activities affecting persons of working age with a peak incidence between 35-55 years of age [41,42]. The injury is followed by months of immobilization and rehabilitation and long-term reduction of tendon function and muscle atrophy is frequently seen. The incidence of acute Achilles tendon ruptures has increased by 17% and 22% among Swedish men and women respectively between 2001 and 2012 [42]. Achilles tendon rupture treatment is either surgical or non-surgical followed by immobilization. Surgical treatment was long considered advantageous as it resulted in a lower risk of re-rupture as compared to non-surgical treatment [51,72]. In the past it was common with months of immobilization in rigid casts following surgery and weight-bearing was not allowed [48]. More recent studies indicate that active rehabilitation using ankle foot orthoses (AFO) that can be removed for range of motion exercise and early weight bearing following surgery, results in higher patient satisfaction, earlier return to pre-injury activities and less reduction in function [18,21]. With more active rehabilitation re-rupture rates following non-surgical treatment have also decreased to almost the same levels as for surgical treatment [41,45,76,94,104]. However, a remaining decrease in patient reported outcome, performance in functional tests, and in the general physical activity level 12-24 months after injury is common following both surgical and non-surgical treatment [75,76,78,104]. In animal models loading of growing and healing tendons has been shown to be beneficial to collagen synthesis and tendon properties [2,17,49]. AFO used following an Achilles tendon rupture should allow sufficient load on the tendon to avoid disuse atrophy and stimulate healing, but protect against accidental overload and injury. In order to study the effect of treatment protocols and rehabilitation exercise on the Achilles tendon a number of methods have been used. Force transducers inserted into the Achilles tendon have been used to quantify tendon force during walking, running and hopping [29,30,55] and Roentgen stereophotogrammetric analysis (RSA) which involves the insertion of tantalum beads into the Achilles tendon has been used to determine strain within the tendon during healing [87]. All of these methods are invasive whereas ultrasound imaging offers a non-invasive method of studying tendons. However, the validity of quantitative assessment of tendon motion and deformation in ultrasound images has so far been limited.

1.2 ACHILLES TENDON ANATOMY

The Achilles tendon is the common tendon of the triceps surae which is formed by the medial and lateral gastrocnemius and the soleus. [73]. The medial and lateral heads of the gastrocnemius have their origin on the posterior aspects of the medial and lateral condyles of femur respectively, whereas the soleus has its origin on the posterior aspect of the head of fibula and the superior fourth of tibia [73]. Since the gastrocnemius passes across both the knee and ankle joints its force generating capacity is dependent on the position of both these joints [15]. The different parts of the triceps surae have different functions, where the soleus's

main function is in standing and slow motion while the gastrocnemius produces rapid movement such as running and jumping [73].

Tendon tissue consists mainly of extracellular matrix containing collagen and proteoglycans, where the tensile strength is mainly provided by the collagen [9]. Tenocytes are the most common cells in tendon tissue [64] and they are typically arranged between the collagen fibers [9]. Collagen type I is the dominant collagen type of healthy tendons, while collagen type III is also present in healing and aging tendons [64]. Tenocytes synthesize procollagen which is exported from the cells and aggregated into tropocollagen [64]. Tropocollagen molecules aggregate in an overlapping and twisting manner to form microfibrils, which are organized in parallel into fibrils, which in turn are organized into fibers, fascicles and finally into tendons [38,64] (Figure 1).

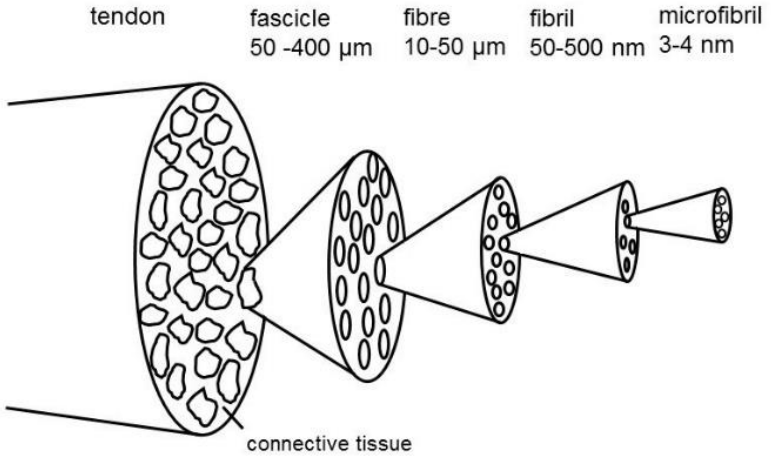

Figure 1. *Hierarchal organization of tendon collagen. (adapted from Handsfield et al [38])*

Tendon fascicles that originate from the aponeuroses of the medial and lateral gastrocnemius and the soleus form the Achilles tendon and the fascicles twist medially before they insert on the calcaneus [6,22,24,98] (Figure 2). Tendon fascicles are separated by loose connective tissue and it has been proposed that the tendon fascicles can slide against each other during motion [9,39]. In support of this theory, a glycoprotein called Lubricin which facilitates tissue sliding has been found at the fascicle interfaces in the distal six cm of the human Achilles tendon [96].

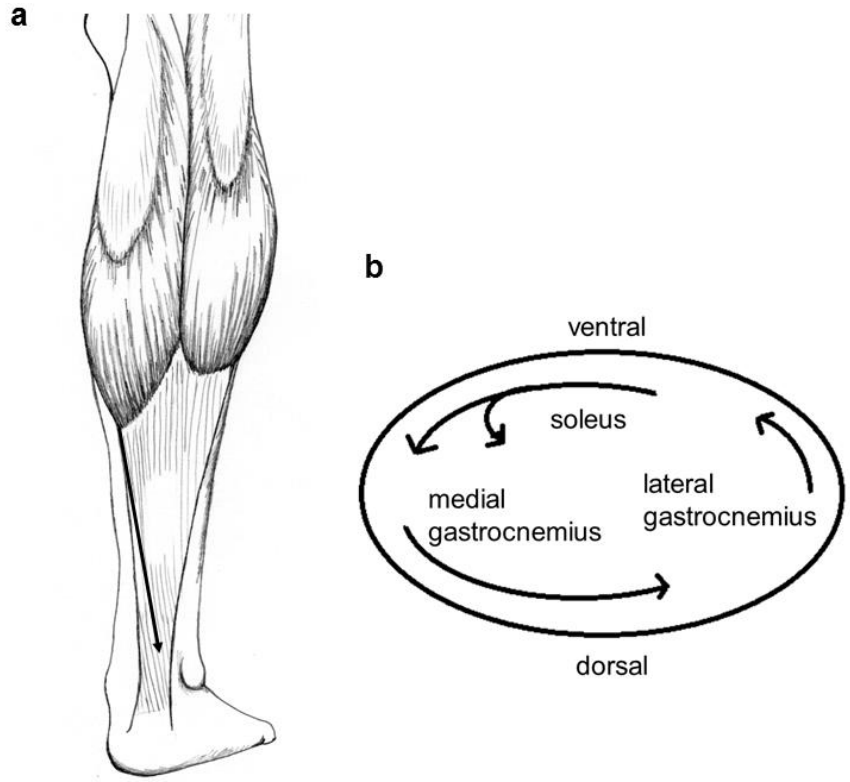

Figure 2a. *Drawing of the right Achilles tendon showing the twist of the tendon fascicles.* ***b.*** *Tendon cross-section showing the orientation of the tendon fascicles during twisting from proximal to distal (adapted from Arndt et al [6].)*

1.3 ACHILLES TENDON BIOMECHANICS

The elastic properties of the Achilles tendon have been studied in-vitro by mounting tendon samples in materials testing machines and straining them to failure while recording tendon elongation and applied force [68]. To enable relevant comparisons between tendon samples of different dimensions, force was normalized to tendon cross-sectional area and expressed as stress (MPa) and elongation was normalized to tendon original length and expressed as strain (%) [68]. Figure 3 shows the relation between stress and strain in a typical tendon. In the initial toe region there is a non-linear relationship between stress and strain where crimped collagen fibers are straightened [68,103]. In the elastic region collagen fibers are stretched, but if stress is released the fibers will return to their initial length [68,103]. In the plastic region fibers start to break and finally the tendon ruptures [68,103]. The slope of the stress strain curve in the linear region is known as the Young's modulus which describes the elastic properties of materials [97].

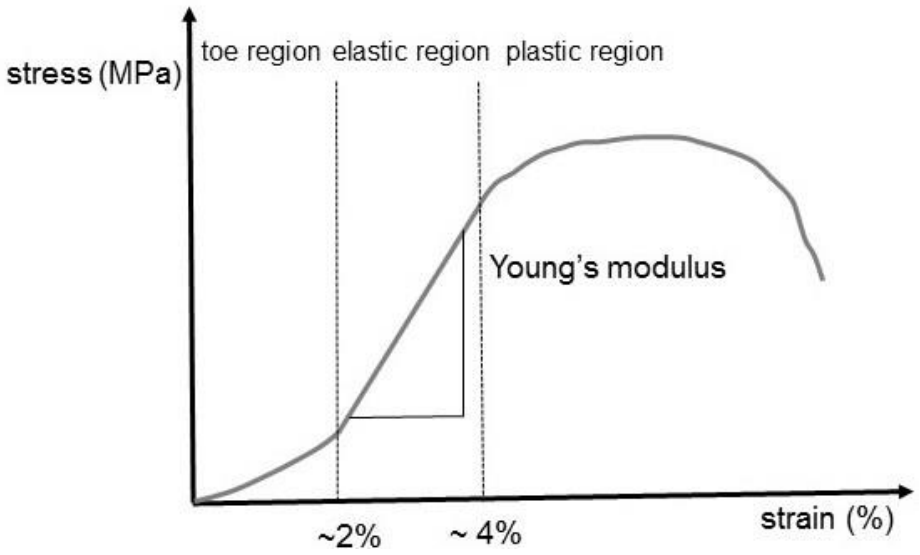

Figure 3. *Stress – strain curve of a tendon. (Based on data from [68,103])*

The elastic properties of the Achilles tendon are utilized during walking and jumping as elastic energy can be stored in the tendon [36,43]. The stance phase of a step lasts between heelstrike and toeoff. Immediately after heelstrike the Achilles tendon will shorten and intratendinous force decreases as the forefoot hits the floor [30,43,55]. During the next part of stance phase, the Achilles tendon is stretched while the tibia moves forward and force starts to build up in the tendon [30,43,55]. During push off the tendon recoils and stored elastic energy is released and contributes to forward motion [36,43,68].

The Achilles tendon is formed by fascicles origination from the three muscles of the triceps surae which may be independently activated, and there is evidence that loading and deformation of the human Achilles tendon is non-uniform during motion [15]. In an in-vitro set up force was measured in medial and lateral parts of the Achilles tendon while different loads were put on the muscles of the triceps surae, and loading of the medial gastrocnemius resulted in higher forces on the medial side of the tendon, whereas loading of the lateral gastrocnemius or a combination of two or three muscles lead to higher forces on the lateral side [5]. The degree of muscle activation and aponeuroses displacement of the soleus and gastrocnemius during isometric plantar flexion depend on the knee angle, so that the gastrocnemius reaches its peak activity [7] and aponeurosis displacement [14] when the knee is close to full extension and the soleus reaches peak activity and aponeurosis displacement when the knee is flexed. In-vitro studies have shown that strain in the Achilles tendon is asymmetrical and varies with different patterns of muscle activation and angles of the calcaneus during loading [61]. Displacement within the distal free Achilles tendon during motion has previously been estimated using ultrasound tracking in vivo [4,31,93]. Arndt et al showed that displacement in deep tendon layers exceeded displacement in superficial layers during passive ankle motion [4] and this non-uniform displacement pattern has also been observed during eccentric Achilles tendon loading [93]. Non-uniform displacement in the

Achilles tendon has also been observed during walking and has been shown to increase with increasing walking speed [31]. Fascicles of the Achilles tendon transmit muscle force independently with little lateral force transmission [39] and it has been suggested that the non-uniform displacement pattern observed in the Achilles tendon during range of motion exercise and walking reflects gliding between tendon fascicles [4,31,39,93]. Fascicle gliding is thought to optimize force transmission of the different components of the triceps surae at different levels of activation and at different angles of the knee and calcaneus [4,15,31].

1.4 TENDON HEALING

Tendon healing after rupture follows the well-established phases of healing, inflammatory phase, proliferative phase and remodeling phase which have been described in animal models [26,99]. During the inflammatory phase (week 1), inflammatory cells gather at the rupture site and through production of cytokines and growth factors they recruit macrophages and tendon fibroblasts [26,99]. In the subsequent phase (1-4 weeks), fibroblasts proliferate and produce fibrillar collagen [17,26]. During remodeling fibroblasts and collagen become oriented in the direction of load [26]. In rat models of Achilles tendon ruptures it has been shown that tendon healing is stimulated by mechanical loading [2,3,17,25]. Continuous weight bearing on the injured limb during free cage activity and intermittent or free exercise on a treadmill resulted in earlier formation of mature repair tissue with thicker and longitudinally organized collagen [17] and tendons with higher stiffness and peak force [2,25], than if the limbs were unloaded or immobilized. In-vitro stretching of human tenocytes has been shown to increase cell proliferation and collagen production [105] which is thought to mediate the beneficial effect of mechanical loading of healing tendon tissue [2]. Ultrasound studies of previously ruptured and surgically repaired Achilles tendons in humans have shown altered echogenicity, scar tissue with disturbed striated appearance and impaired gliding between the tendon and surrounding tissue several years after injury [11,71,84]. Knowledge of the effect of mechanical loading on the morphology of healing human Achilles tendons is limited, but in patients with Achilles tendon rupture early active loaded plantarflexion exercises have shown to result in healed tendons with higher elastic modulus [86]. More active rehabilitation protocols with early range of motion exercises following Achilles tendon ruptures seem to improve tendon properties and result in reduced re-rupture rates [51,94], but impaired plantarflexion function compared to the uninjured leg is still common [76,78,104].

1.5 ANKLE FOOT ORTHOSES

An ideal AFO to be used following an Achilles tendon rupture should allow sufficient load on the tendon to stimulate healing and avoid disuse atrophy, but protect against accidental high loads that may damage the healing tendon [1,50]. Elongation of the Achilles tendon following rupture has been correlated with poor outcome [47,87,89] and should also be prevented. AFO are thought to reduce tension loading in the Achilles tendon by limiting dorsiflexion of the ankle and to reduce active loading by reduction in muscle activity in the lower leg [1,50]. There are a few principally different designs of AFO commonly used in

treatment protocols for Achilles tendon ruptures. One design has a rigid outer shell and a rocker-bottom sole and is commonly used in combination with heel wedges to achieve the desired ankle angle [78,104] (Figure 4a). Another design of AFO has an adjustable foot-plate on a hinge that can be set to different ankle angles and which allows limited range of motion [76,101] (Figure 4b). A third AFO design functions as a dorsal brace restricting excessive dorsiflexion while leaving plantarflexion unrestricted [47,67] (Figure 4c). There are only a few studies of the biomechanical properties of AFO and how they affect the Achilles tendon and the lower leg muscles during walking. Muscle activity of the soleus and gastrocnemius has been shown to decrease compared to unbraced walking when the rigid AFO was used [46], and was further decreased with each addition of a heel wedge [1]. Plantar pressure has been measured inside the rigid AFO design and was used to calculate ankle moments [85] and forefoot pressures [50] which were both shown to decrease during walking in the rigid AFO. In these studies force or deformation in the Achilles tendon were not directly measured. In study I of this thesis the function of an adjustable AFO was investigated using a force transducer in the Achilles tendon together with EMG measurements of activity in the triceps surae [33]. EMG activity of the soleus decreased with increasing dorsiflexion limit as had previously been shown for the rigid AFO design, but gastrocnemius activity showed a different pattern and force in the Achilles tendon increased with increasing dorsiflexion limit [33]. This lead to the hypothesis that principally different designs of AFO may have different effects on the healing Achilles tendon. No studies of the biomechanical effects of the dorsal brace were found. A study comparing the biomechanical properties of different AFO designs with respect to EMG activity of the lower leg, plantar pressure and tendon deformation is lacking.

Figure 4. *Three commonly used AFO designs.* ***a*** *rigid AFO* ***b*** *adjustable AFO* ***c*** *dorsal brace.*

1.6 FORCE MEASUREMENTS

1.6.1 Indirect force calculations

Using the balance of moments about the ankle joint, Achilles tendon force can be calculated from plantar force measurements. Ankle joint center of rotation, ground reaction force (GRF) and the length of the moment arms of the GRF and force in the Achilles tendon need to be determined (Figure 5). Ankle joint center of rotation and lengths of moment arms can be determined on X-ray or estimated from surface anatomy. In these calculations the contributions from plantarflexion muscles which do not exert force via the Achilles tendon are assumed to be negligible [7,35]. A further limitation of this method during dynamic measurements, is that ankle moment arms change as the ankle angle changes [35].

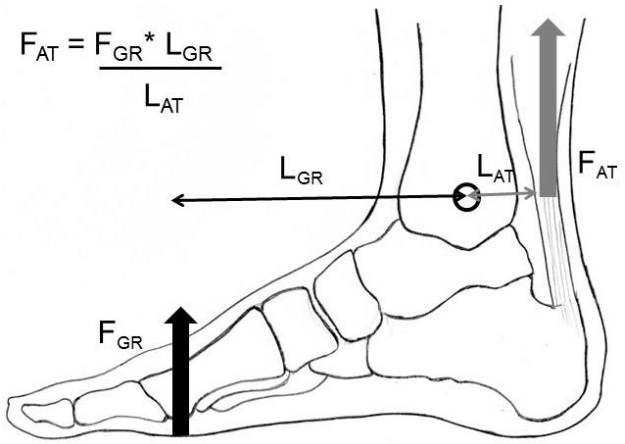

Figure 5. *Calculation of Achilles tendon force (F_{AT}) when the center of rotation, ground reaction force (F_{GR}), and moment arm lengths (L_{GR} and L_{AT}) are known.*

1.6.2 Buckle force transducers

The first methods for measuring in-vivo forces in the human Achilles tendon were developed in the 1980s. [53,83]. The buckle transducers used at that time consisted of a stainless steel frame which was fastened on the Achilles tendon during open surgery [56]. Tensile forces in the tendon resulted in forces on the buckle transducer which were recorded by strain gauges attached to the frame [37]. Force sensors used for experiments on tendons needed to be calibrated against some known force. In animal experiments this was usually done at the end of the experiment when the tendon was cut and connected to a dynamometer, after which transducer output could be calibrated against applied forces under static or dynamic conditions [53]. In human studies calibration was more difficult and relied on indirect force calculations [28,53]. Differences in transducer placement, ankle angle, magnitude of force and force rate between calibration and experiment are potential sources of error [37,53]. The introduction of buckle transducers enabled measurements of Achilles tendon forces during

activity, including walking, running, hopping and cycling [53]. However, the requirement for open surgery was a disadvantage limiting the use of this technique [54].

1.6.3 Optic fiber force transducers

Optic fibers are designed to efficiently transmit light from a light source to a receiver. Komi et al developed a technique to use an optic fiber as a force sensor in tendons [54]. This method utilizes the Poisson effect, which describes how materials stretched in the axial direction tend to contract proportionally in the transverse direction [97]. The optic fiber was inserted through the tendon and connected to a light source and a receiver. As the tendon was loaded it was strained in the longitudinal direction and proportionately decreased its thickness, which resulted in compressive or bending forces on the optic fiber which in turn modulated the intensity of the transmitted light [54]. In an in-vitro model using rabbit Achilles tendons it was demonstrated that the optic fiber output signal showed a linear relationship with load on the tendon under static conditions [54]. In the human application of this technique the optic fiber output signal was calibrated against measured ankle plantarflexion torque at different levels of muscle contraction [29,30]. Force in the Achilles tendon was calculated and plotted against the optic fiber signal to obtain a calibration coefficient for each study person [29,30]. The advantage of the optic fiber technique is that it is minimally invasive compared to use of buckle transducers [30,83]. Potential sources of measurement error include migration of the fiber through the tendon, non-linear relationships between tendon loading and optic fiber output under dynamic conditions and differences in loading rate between calibration and measurements [28,83]. Skin movement over the tendon may cause artefacts and measurement errors but reports of the magnitude there of vary greatly [27,29].

1.7 ULTRASOUND IN BIOMECHANICS

1.7.1 Ultrasound imaging

Ultrasound images are generated by beams of high frequency sound waves which are transmitted into the body and reflected against interfaces between tissues. Ultrasound transducers used in medicine, work both as transmitters and receivers and contain rows of piezoelectric elements. Piezoelectricity is the property of materials to produce electric charge in response to mechanical deformation and conversely to deform in response to an applied electrical current. When an alternating current is applied to the piezoelectric elements of the ultrasound transducer, they start to vibrate at the same frequency as the applied current. The vibrations are transferred through the surface of the transducer into the body and then propagate as mechanical waves into the tissue. Different materials have different abilities to propagate sound waves, a phenomenon known as acoustic impedance [44]. As propagating sound waves reach interfaces between tissues with different acoustic impedance a proportion of the wave will be reflected, and the degree of reflection is proportional to the difference in acoustic impedance. The difference in acoustic impedance is large between air and soft tissue [44], and therefore air between the transducer and body surface or within organs will result in

almost total reflection and no further propagation of the wave into the tissue. Transmitted pulses are reflected back to the transducer where they are received by the piezoelectric elements and converted to electrical current. Information about the time delay and intensity of the echo is used to determine the position and acoustic properties of the reflecting tissues. This procedure is repeated for adjacent scan lines and eventually each pixel in the image is assigned a brightness according to its corresponding echo.

Not all ultrasound waves propagating through tissue will be reflected directly back to the transducer. If the reflecting surfaces are uneven or at an angle with the propagating wave, part of the wave will be scattered. Small objects with the same size as the ultrasound wavelength will also scatter the wave. Scattered waves will interfere, either by constructive interference where waves add in intensity or by destructive interference where waves cancel each other out. This gives rise to the random speckle pattern of bright and dark spots in ultrasound images (Figure 6).

The spatial resolution of an ultrasound image is the ability to discriminate between two adjacent objects. It is commonly divided into three components, axial resolution along the ultrasound beam, lateral resolution along the width of the ultrasound transducer and elevational resolution along the thickness of the transducer. The axial resolution is dependent on the length of the transmitted pulse which in turn is dependent on the sound wavelength and the number of cycles in the pulse. In order for two echoes from adjacent interfaces to be discriminated, they need to be separated by at least half the pulse length or they will fuse to one. The lateral and elevational resolution are dependent on the width of the ultrasound beam. Echoes from two objects which are separated by less than a beam width will be perceived as one. The axial resolution is higher than the lateral resolution as it is easier to generate short rather than narrow ultrasound pulses. However, tissue absorption of the sound wave increases with shorter wavelengths (higher frequencies), so there is an upper limit to the frequencies depending on the desired scan depth [44]. The temporal resolution of an ultrasound system is the number of images or frames generated per second, which is dependent on the size of the scanned field, the number of scanned lines and focus points. Ultrasound is well suited for investigation of tendons as they generally run close to the body surface and thereby allow high axial resolution images using high frequency transducers.

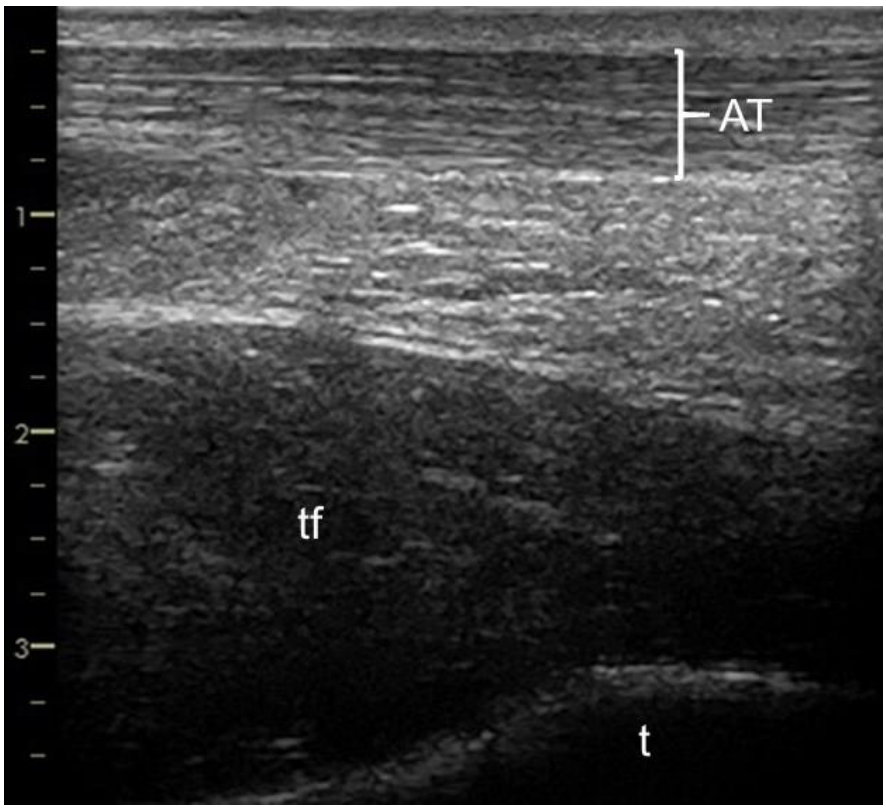

Figure 6. *A long axis ultrasound image of a human Achilles tendon with the typical striated speckle pattern. The axis on the left indicates depth in cm. AT = Achilles tendon, tf = toe flexors, t = tibia.*

1.7.2 Ultrasound tracking of the musculotendinous junction

A technique for estimation of Achilles tendon length and strain during motion using ultrasound tracking of the musculotendinous junction in the calf in combination with motion analysis has been described and used in a variety of applications [13,34,43,62,69]. In this technique an ultrasound acquisition of the junction of the Achilles tendon and the distal insertion of the gastrocnemius or soleus muscles is performed. The position of the musculotendinous junction is tracked from frame to frame in the ultrasound sequence. Motion analysis is used to track the relative positions of the ultrasound transducer and the Achilles tendon's point of insertion in the calcaneus. By combining the results of the ultrasound tracking and the motion analysis, the change in position of the musculotendinous junction relative to the calcaneal tendon insertion can be calculated over time. Strain can then be calculated as length change divided by resting length. This technique provides knowledge of motion and strain in the full length of the Achilles tendon [63], but it cannot be used for estimation of displacement or strain in different regions of the tendon as tracking is limited to the proximal and distal ends.

1.7.3 Ultrasound speckle tracking

Ultrasound speckle tracking uses the random speckle pattern present in all ultrasound images for tracking specific regions of tissue, instead of using anatomical landmarks. The speckle pattern is relatively constant between consecutive frames of an ultrasound sequence and can therefore be used for tracking motion. Motion tracking is performed by computer post processing of the images using algorithms which are applied to ultrasound sequences after acquisition. A small area known as a kernel is selected in the first frame of a motion sequence. The algorithm will then move to the second frame and search for an area of the same size as the original kernel where the best match in speckle pattern is found. This is achieved by calculating a similarity measure comparing the brightness of the pixels in the original kernel to that of each target kernel. The search for the best matching kernel is limited to a search area the size of which is determined by the expected velocity of the estimated motion. The position of the kernel with the best match is chosen as the new kernel position, and displacement is calculated between the original kernel and the new kernel. This procedure is repeated for all kernels in frame one and frame two with some degree of overlap, and then for all consecutive frames in the ultrasound sequence. Average displacement can then be calculated within a chosen region of interest (ROI), and can be compared to other regions. Strain can be calculated as the difference in displacement between regions but is more challenging as it is based on fewer motion estimates [92]. The similarity measure used for matching kernels, the size and shape of kernels and search areas and the degree of kernel overlap is determined by the features of the speckle pattern and what magnitude and velocity of motion is to be analyzed.

Speckle tracking was first introduced in echocardiography for motion analysis of the myocardium [40,82] and to date, the commercially available speckle tracking algorithms are developed for use in echocardiography. There are challenges involved in applying the technique to tendon tissue. As the relevant motion of tendons often occurs along the surface of the body, motion estimations must be made perpendicular to the ultrasound beam and therefore with a lower image resolution. The speckle pattern of tendons is striated in the direction of motion which makes it more difficult to identify kernels with a unique pattern compared to the more spotted appearance of the myocardium [59]. Furthermore, measurement accuracy needs to be higher in order to measure the comparatively small displacement and strains expected in the Achilles tendon during motion [43,63]. The advantage of commercial speckle tracking algorithms is that the same technique is available to all which facilitates comparison of results. Yoshii et al evaluated a commercial algorithm for estimation of displacement in finger flexor tendons and showed a moderate correlation between estimated displacement and reference displacement and a tendency for underestimation of displacement by speckle tracking [106]. Another commercial algorithm has been used for estimation of displacement in different layers of the Achilles tendon and found displacement to be non-uniform [4]. It would be interesting to measure strain in tendon tissue as it is thought to be related to injury [65,66], but as mentioned previously strain estimation is more challenging than estimation of displacement [92]. Measurement

parameters are not specified in commercial algorithms and cannot be adjusted by the user for new applications. Therefore in-house speckle tracking algorithms which are not available to all users have been developed and evaluated for estimation of displacement [19,32,59] and strain [12,20] in tendon tissue.

1.8 ELECTROMYOGRAPHY

Muscle fibers contract in response to stimulation by motor neurons. At rest there is a resting potential across muscle cell membranes maintained by ion pumps. Activation of a motor neuron leads to depolarization of the membrane and if the depolarization reaches a threshold value, membrane conductance for Na^+ and K^+ increases which causes a rapid change in membrane potential [10]. This in turn leads to depolarization of other parts of the membrane and an action potential that travels down the muscle fiber. After the action potential has passed, the resting potential is rapidly restored. Muscle force output during contraction is modulated by gradual changes in the number and size of activated motor neurons and their firing rates [10]. Electromyography (EMG) measures the sum of potentials from adjacent motor units between electrodes, and the amplitude and density of the EMG signal reflects motor unit recruitment [57]. EMG can be sampled using surface electrodes which are glued on the skin or intramuscular needle electrodes which are used for EMG sampling from deeper muscles. Raw EMG signals contain both positive and negative spikes and have a mean value of zero (Figure 7a). Spike amplitudes in the raw EMG signal show great variation as they are the result of random interference by potentials from neighboring motor units and individual peak values may not be representative for the general signal trend [57]. Therefore it is common to find the absolute value of the raw signal (Figure 7b) and to use some form of smoothing (Figure 7c) before finding mean or peak values. The amplitude of EMG signals varies with electrode placement in relation to motor end plates and tissue conductivity, which in turn depends on thickness of subcutaneous layers, temperature and contact between electrodes and skin [57]. These factors vary between individuals and also within individuals between different measurement occasions and therefore direct comparison of EMG amplitudes is not meaningful. Instead it is common to normalize amplitudes against muscle activity during some reference activity and present results as percentages[57]. Reference EMG is collected at the same occasion under the same conditions as the actual measurements. EMG during maximum voluntary contraction (MVC) of each muscle is a common reference. However, study participants' ability of to perform MVCs of single muscles varies, especially if they are not well trained or injured and then MVCs are not comparable between participants [57]. Instead EMG during some familiar activity can be used as reference. There is natural variation in the duration of a complete motion cycle, for example a stride, within individuals and between individuals. Peak muscle activity will therefore occur at different time points. Direct averaging of EMG curves will result in combination of muscle activities from different phases of the motion cycle which may modify curve shapes. To avoid this, it is recommended to normalize time to the duration of each motion cycle and present data as a fraction of the complete cycle [57].

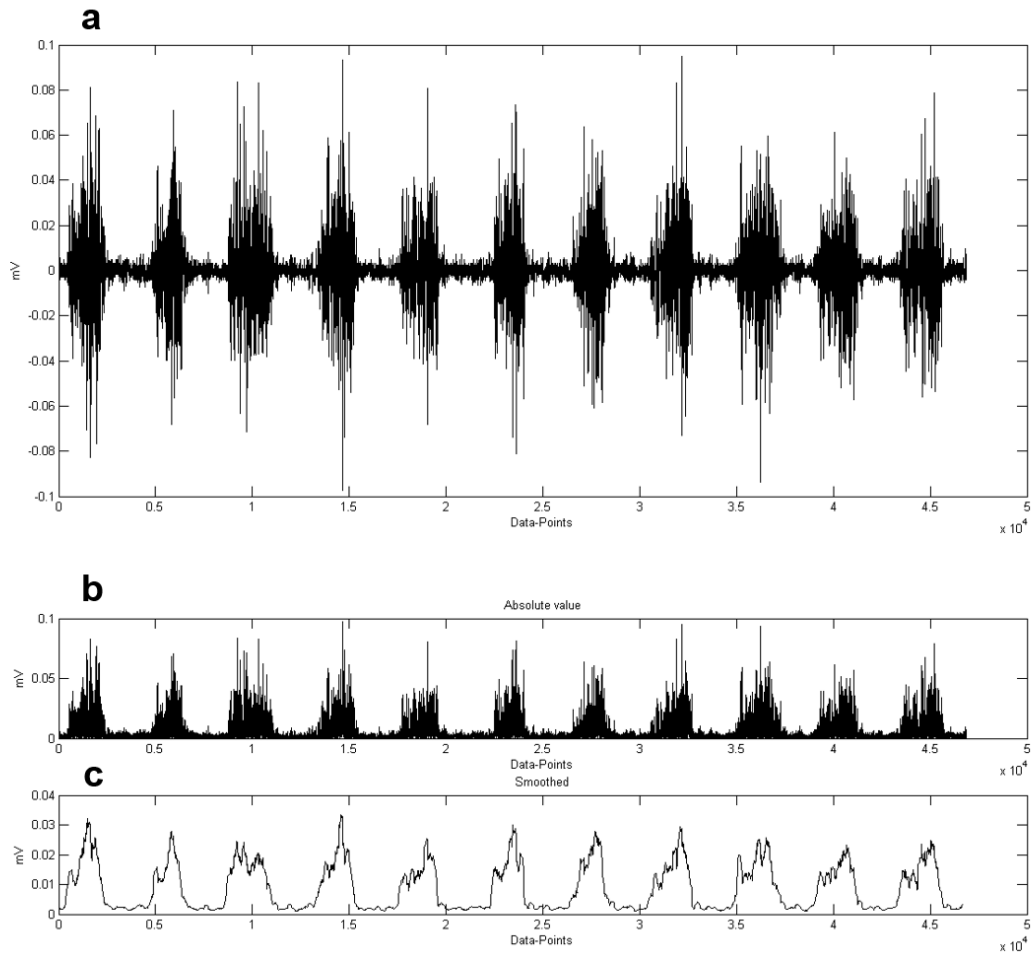

Figure 7. *EMG of the Soleus muscle during slow walking with a sampling frequency of 3000 Hz, a) raw unprocessed EMG signal, b) absolute value of raw EMG signal, c) smoothed curve using moving average over 200 datapoints (≈67 ms).*

1.9 GROUND REACTION FORCE AND PLANTAR PRESSURE MEASUREMENT

GRF and plantar pressure can be measured using platform systems or insole systems. Force platforms are advantageous in that they can measure both vertical and shear components of GRF with high resolution [79] but a limitation is that they are stationary. Insole systems have pressure sensors built into insoles which are lightweight and mobile and can be worn inside shoes and AFO. There are different types of sensors including capacitive sensors and resistive sensors which react to pressure by a change in capacitance or resistance which in turn modulates the voltage in a circuit in proportion to the applied pressure [81]. Piezoelectric materials are also used as pressure sensors as they react to compression by producing a proportional charge [81]. Prior to use, sensor output is calibrated against a known pressure [79]. Most commercial insole systems can only measure force perpendicular to the sensors [79,95] and no shear forces. The spatial resolution of plantar pressure insoles is dependent on

the size and number of sensors and the temporal resolution is dependent on sampling frequency [79,81]. To increase reliability of pressure measurements it is recommended to use an average of several walking trials [8,79]. For comparison of plantar pressures between different regions of the foot or for the same region under different walking conditions, it is common to use an average of several sensors. To increase comparability between studies there are guidelines that recommend how to define different foot regions [8]. As plantar pressure is affected by body weight and shoe size it can be suitable to normalize data before comparison between participants.

2 AIMS

The general aims of this thesis were to improve understanding of how injury and use of AFO affect load and deformation within the Achilles tendon and to adapt and evaluate an ultrasound based method for studying the biomechanics of the Achilles tendon during motion. The specific aims of each study are listed below.

Study I To determine whether Achilles tendon load and lower leg muscle activity would decrease with increased restriction of dorsiflexion in an AFO with an adjustable foot plate.

Study II To investigate the feasibility of a commercial ultrasound speckle tracking algorithm for assessing strain in tendon tissue in an in-vitro experimental set up.

Study III To use ultrasound speckle tracking to compare tendon motion patterns between uninjured and surgically repaired Achilles tendons and to evaluate an in-house developed speckle tracking algorithm for analysis of displacement in tendon tissue.

Study IV To combine ultrasound speckle tracking, electromyography of the lower leg muscles and plantar pressure measurement to investigate how the Achilles tendon is affected by the use of three different designs of AFO with varying degrees of ankle dorsiflexion limitation.

3 PARTICIPANTS AND METHODS

Table 1 shows an overview of the four studies included in this thesis regarding study populations and measurements used.

Thesis overview

	Study I	Study II	Study III	Study IV
description	investigation of an adjustable AFO	evaluation of a commercial STA for estimation of strain	1) evaluation of an in-house STA for estimation of disp 2) comparison of injured and uninjured AT	investigation of an adjustable AFO, a rigid AFO and a dorsal brace
participants	healthy participants	one patient	AT rupture patients	healthy participants
number of participants (♀/♂)	8 (5/3)	none	11 (1/10)	16 (8/8)
tendon samples	no	3 porcine grafts 1 human graft	2 porcine feet, soft tissue intact	no
force measurement	optic fiber	no	no	no
speckle tracking	no	in-vitro strain evaluation	in-vitro disp evaluation in vivo disp estimation	in-vivo disp estimation
EMG	gcm, sol, ta	no	no	gcm, gcl, sol, ta
GRF / plantar pressure	force plate system	no	no	insole system

Table 1. *Overview of the study participants, tendon samples and measurement methods used in the different studies. AFO = ankle foot orthoses, AT=Achilles tendon, STA = speckle tracking algorithm, disp = displacement, GRF = ground reaction force, gcm = gastrocnemius mediale, gcl = gastrocnemius laterale, sol = soleus, ta = tibialis anterior*

3.1 PARTICIPANTS

3.1.1 Study I

Eight healthy participants, five female and three male with mean and standard deviation (SD) age: 24 ± 3 years, height: 170 ± 6 cm and weight 65 ± 8 kg participated in this study. The study was approved by the human ethics committee of the Karolinska Institute and by the ethics committee of the University of Jyväskylä; Finland. All participants gave written informed consent.

3.1.2 Study II

A human Achilles tendon allograft was used in this study. The tendon allograft with calcaneal bone attachment was harvested during a subacute lower leg amputation due to arteriosclerotic

ulcers. The Stockholm Regional Ethics Committee approved the study and the patient gave written informed consent.

3.1.3 Study III

Between February 2007 and April 2008, 68 patients were surgically treated for an Achilles tendon rupture at the Karolinska University Hospital Huddinge. Persons with age < 18 years or > 65 years, bilateral injury, re-rupture, post-operative infection or no longer living in Stockholm were excluded. Remaining persons were informed about the study by mail and eleven persons, one female and ten male with mean and SD age: 50 ± 9 years, height: 177 ± 10 cm and weight 82 ± 16 kg agreed to participate. All patients were treated surgically and post-operatively they were immobilized in a plaster cast in equinus for two weeks followed by immobilization using an adjustable AFO for six weeks. Partial weight bearing was allowed two weeks after surgery and weight bearing as tolerated after six weeks. The Stockholm Regional Ethics Committee approved the study and participants gave written informed consent.

3.1.4 Study IV

Sixteen healthy participants were recruited for this study, eight females mean and SD age: 44 ± 3 years, height: 170 ± 5 cm, and weight: 66 ± 10 kg and eight males mean and SD age: 45 ± 3 years, height: 183 ± 7 cm and weight: 82 ± 13 kg. The participants' ages were chosen to match patients suffering an Achilles tendon rupture. The study was approved by the Stockholm Regional Ethics Committee and participants gave written informed consent.

3.2 EXPERIMENTAL SET UP

3.2.1 Evaluation of speckle tracking strain estimation (study II)

A commercially available speckle tracking algorithm was evaluated for strain estimation in tendon tissue in an in-vitro set up. The algorithm was evaluated in three steps, first on a tendon phantom, secondly on three porcine flexor tendons, and lastly on a human Achilles tendon allograft. The objective of the first step was to test the performance of the algorithm under conditions similar to those expected in the Achilles tendon during walking regarding image resolution, depth, dimensions, strain and strain rates. A polyvinyl alcohol (PVA, Sigma-Aldrich, St Louis, USA) phantom with dimensions similar to the human Achilles tendon (115 x 15 x 5 mm) with addition of graphite powder (Merck, Darmstadt, Germany) to simulate a speckle pattern was molded. The PVA phantom was mounted in a materials testing machine (ElectroPuls E3000, Instron, Norwood, USA) which was programmed to simulate strain in the Achilles tendon during walking. A sensor on the motor shaft of the materials testing machine recorded displacement of the upper attachment of the PVA phantom, and reference strain was obtained by dividing lengthening by initial length. Ultrasound acquisitions of the PVA phantom were made during motion and ten strain cycles were recorded. In the second step of the evaluation, the speckle tracking algorithm was tested on porcine flexor tendons which have a speckle pattern resembling that of human Achilles

tendons. Fresh frozen porcine feet were purchased at the local food store and the flexor digitorum tendons with attached distal phalanx were removed. The proximal tendon end was attached in the materials testing machine using a pressure clamp and the distal bony attachment was molded into a fiberglass block which was screwed into the bottom plate of the materials testing machine. The tendons were then strained following the same protocol as for the PVA phantom while ultrasound acquisitions were made. In the final step the algorithm was tested on a human Achilles tendon allograft. The tendon allograft was mounted in the materials testing machine (Figure 8a) and strained in the same manner as the porcine tendons while ultrasound acquisitions were made.

3.2.2 Evaluation of speckle tracking displacement estimation (study III)

An in-house developed speckle tracking algorithm was evaluated for estimation of displacement in tendon tissue. The in-vitro set up described in 3.2.1 was designed as a model to provide a reference strain and not displacement. A limitation of the set up was that the reference strain was calculated from the motion of the materials testing machine, which due to possible slipping at the pressure clamps and inhomogeneity in tendon properties may not have been a true reference. For these reason, another model similar to that previously described by Korstanje et al [58,59] was used for displacement evaluation in study III. Two fresh frozen porcine feet were used. A 5x5 mm aluminum plate was inserted into a flexor digitorum tendon of each foot from the side, leaving skin and soft tissue covering the tendon. Sutures (no 2 Ethibond, Ethicon, Livingston, Scotland) were attached to each tendon end. The proximal tendon suture was attached to a steel wire, which in turn was attached to the materials testing machine (Figure 8b). A 500g weight was attached to the distal tendon suture. The materials testing machine was programmed to displace the tendon 5 mm, 10 mm and 15 mm at 5 mm/s, 10 mm/s and 15 mm/s. Ultrasound imaging of five trials for each displacement and velocity were acquired. Due to mechanical losses in the set up, the displacements and velocities known from the materials testing machine could not be used as references [59]. Instead both ends of the aluminum plate were manually tracked in the ultrasound sequence frame by frame, resulting in two displacement curves for each trial. Mean peak displacement was used as reference.

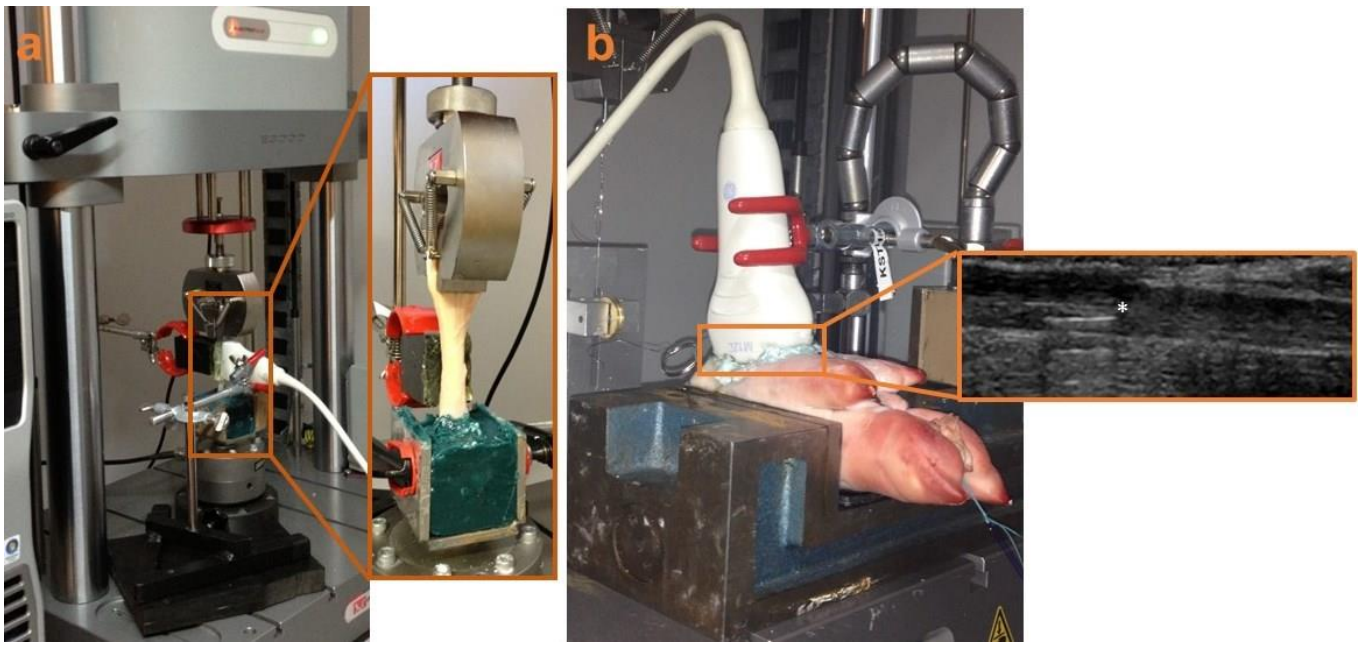

Figure 8a. *Experimental set up for evaluation of speckle tracking strain estimation (study II). A human tendon allograft mounted in the materials testing machine with the ultrasound transducer fixed on the tendon. Insert: human tendon allograft.* ***b.*** *Experimental set up for evaluation of speckle tracking displacement estimation (study III). A porcine foot mounted in the materials testing machine with the ultrasound transducer fixed over the tendon. Insert: ultrasound image of a porcine flexor tendon with inserted aluminum plate *.*

3.2.3 Examination of Achilles tendons following surgical repair (study III)

Eleven patients were examined on average 19 ± 4 months after surgical repair of an Achilles tendon rupture. They answered a general questionnaire and the Achilles tendon rupture score (ATRS) [77]. Patients lay prone on an examination table with both feet hanging over the end. Ankle range of motion was measured bilaterally using a goniometer. Three repeated Thompson's squeeze tests were then performed [90,100] on the surgically repaired and uninjured tendons respectively. Patients then performed three repeated active ankle dorsiflexions between resting position and maximum dorsiflexion on both sides. Ultrasound images of the Achilles tendons were acquired during both motions.

3.2.4 Investigation of ankle foot orthoses (study I and IV)

In this thesis three different designs of AFO were investigated at different ankle angles, with regards to their effect on force and deformation in the Achilles tendon, muscle activity of the lower leg and plantar pressures. The first design was a rigid AFO with air bladders and a rocker bottom sole (Rebound Air Walker, Össur, Reykjavik, Iceland) where ankle angle was adjusted using zero, two or three 10 mm heel wedges (Study IV). The second design was an adjustable AFO in which the ankle angle could be set using an articulating hinge. It was investigated in study I (articulating walker, DeRoyal Europe Inc, Ireland) using three settings, dorsiflexion limited to 10° dorsiflexion with unrestricted plantarflexion, dorsiflexion limited

to 10° plantarflexion with unrestricted plantarflexion and locked at 20° plantarflexion with no range of motion. In study IV a similar AFO (ROM Walker, DJO Global, Vista, USA) was tested with settings dorsiflexion limited to 10º dorsiflexion, 10º plantarflexion or 30º plantarflexion respectively, while plantarflexion was unrestricted. This AFO design with similar settings was part of the clinical treatment protocol used for the patients examined in study III. The third type of AFO was a dorsal brace which was prepared for each participant using 10 layers of casting tape (Scotchcast Plus, 3M Health Care, St Paul, USA) with an ankle angle of 90°. It was fastened on the leg using cohesive bandage (Mollelast haft, Lohmann & Rauscher International GmbH & Co, Rengsdorf, Germany) and worn inside a running shoe. The dorsal brace was tested using zero or one 10 mm heel wedge. Both the rigid and the adjustable AFO were adjusted to make room for an optic fiber force transducer (Study I) or ultrasound transducer (Study IV). For the AFO conditions participants wore a running shoe on the contralateral foot to compensate for leg length differences. All participants also walked without an AFO and this condition will be referred to as barefoot walking.

3.2.4.1 Study I

In study I the adjustable AFO was investigated. Participants walked twice at self-selected speed along a 10 m force platform, barefoot without an AFO and wearing the AFO with the three settings described previously. Achilles tendon force was measured using an optic fiber force transducer. Muscle activity for the medial gastrocnemius, soleus and tibialis anterior and GRF were recorded.

3.2.4.2 Study IV

In study IV the rigid AFO, the adjustable AFO and the dorsal brace were investigated. Participants walked and ran on a treadmill at 2 km/h and 10 km/h respectively, barefoot without an AFO and wearing the AFO with the settings described above. Motion in the Achilles tendon was recorded using ultrasound, muscle activity was recorded for the medial and lateral gastrocnemius, soleus and tibialis anterior and plantar pressure was measured using an insole system (Figure 9). Three 15 s recordings were made for each walking condition.

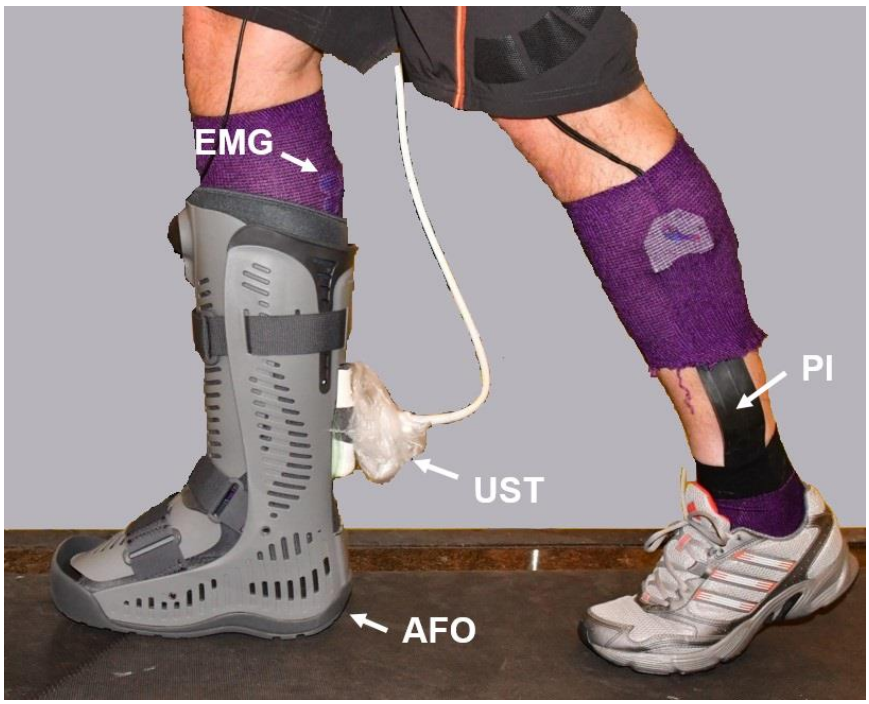

Figure 9. *Experimental set up for functional evaluation of different AFO designs in study IV. EMG = emg electrodes, UST = ultrasound transducer, PI = pressure insole, AFO = rigid AFO*

3.3 DATA COLLECTION AND ANALYSIS

3.3.1 Optic fiber force measurement

Achilles tendon force and rate of force development was measured using an optic fiber force transducer during walking barefoot and in an adjustable AFO (Study I). Before fiber insertion the skin over the Achilles tendon was anesthetized using EMLA cream (Astra Zeneca, Sweden). Participants lay supine with the right leg strapped to an ankle dynamometer with a 90° ankle angle and a 100° knee angle (Figure 10a). As part of the calibration procedure participants were instructed to perform three ankle plantarflexions at MVC while ankle torque was measured. Thereafter the midportion of the Achilles tendon was palpated and a 1.1 mm cannula was inserted through the tendon. The optic fiber (polymethyl methacrylate, thickness: 0.5 mm, length 1m, PRG series, Toray Inc, Japan) was passed through the cannula, and then the cannula was removed leaving the fiber in the tendon (Figure 10b). The ends of the fiber were connected to a light-emitting diode (GaAIAs semiconductor, HFBR-1414, Hewlett Packard, Palo Alto, USA) and a photodiode receiver (HFBR-2414, Hewlett Packard). For calibration participants performed three ankle plantarflexions at 10%, 20% and 30% of MVC respectively, while ankle torque and optic fiber output were recorded. Achilles tendon force was calculated and the optic fiber signal was plotted against the calculated force and by using linear regression a correlation was found for each participant. Optic fiber signals were then recorded during barefoot walking and with the AFO set at three different ankle angles. Raw optic fiber data was converted into Achilles tendon force using the calibration

factor for each participant and then imported into Origin 6.1 (Microcal Software Inc, Northampton, USA). Peak Achilles tendon force during stance phase was manually identified for all steps in a walking trial, ignoring the first and last steps to avoid acceleration and deceleration effects. Mean peak force was calculated for all participants and walking conditions. To make force comparisons between participants relevant, the peak values were normalized to body weight. Rate of force development was calculated as the slope of the force-time curve during stance phase between the minimum and maximum values. Average rate of force development was then found for all participants and walking conditions.

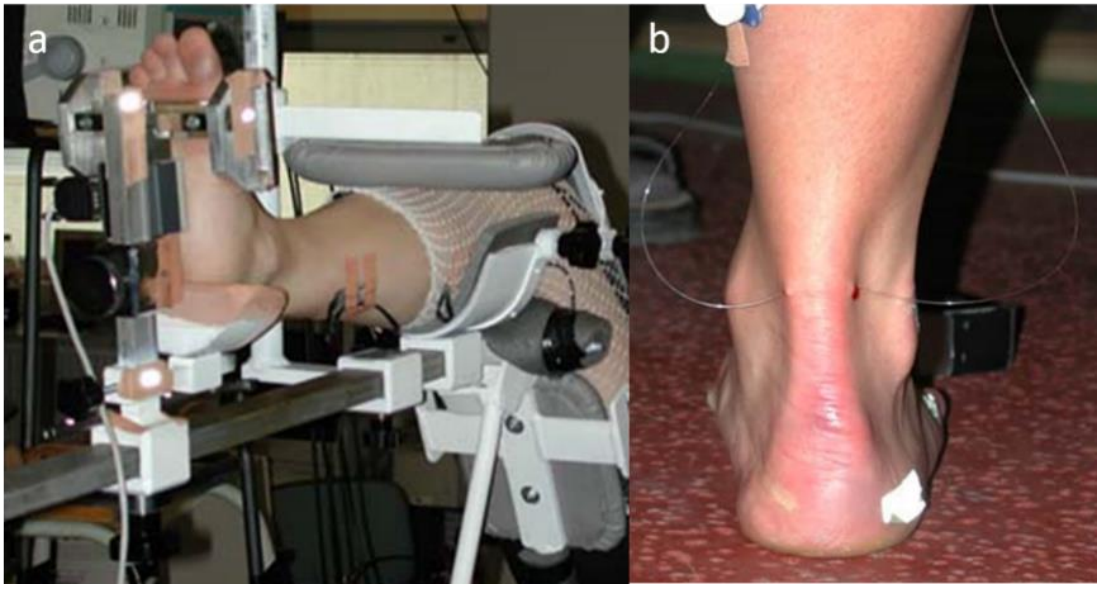

Figure 10a. *Set up for calibration of the optic fiber output signal to ankle plantarflexion torque.* ***b.*** *Optic fiber in place in the Achilles tendon of one participant.*

3.3.2 Electromyography

In study I and IV EMG was recorded for the medial gastrocnemius, soleus and tibialis anterior and in study IV the lateral gastrocnemius was also added. Bipolar surface electrodes were used and they were positioned over the muscle belly of the medial and lateral gastrocnemius and tibialis anterior during contraction. For the soleus a position below the muscle bellies of the medial and lateral gastrocnemius was chosen. To minimize impedance, skin was shaved and cleaned with alcohol before electrode placement. Electrodes, amplifiers and cables were secured with net bandages or compressive stockings to avoid loosening or movement artifacts. Sampling frequencies were 1013 Hz and 3000 Hz for study I and IV respectively. For further processing EMG raw data were imported into Origin 6.1 for Study I and Matlab (R2014a, Math Works Inc., Natick, USA) for study IV. EMG raw data were rectified using absolute values. For study I overshooting values were removed, whereas in study IV ten steps without overshooting values were chosen for analysis. Smoothing was

done using a 200 points moving average filter. In study I EMG for each muscle was normalized to mean muscle activity during barefoot walking. In study IV EMG during MVC was recorded for gastrocnemius, soleus and tibialis anterior and the intension was to normalize EMG data to MVC. During data analysis a large variation in the quality of MVC between participants was noted, and therefore mean peak muscle activity during barefoot running at 10 km/h was chosen for normalization instead. Peak EMG values were identified on the resulting curves. In study I mean peak activity and 95% confidence intervals were calculated for medial gastrocnemius, soleus and tibialis anterior for all participants and walking conditions. Mean EMG curves were reported for one participant. In study IV mean and SD of peak activity was calculated from ten steps for all participants and all walking conditions, for the medial and lateral gastrocnemius, soleus and tibialis anterior. To adjust for differences in step length, all EMG curves were interpolated to a fraction of the step before mean EMG curves were calculated.

3.3.3 Ultrasound image acquisition

Ultrasound image acquisition in the experimental set up in study II was conducted using an 8L-RS linear array transducer (GE Healthcare, Horten, Norway) connected to a Vivid*i* ultrasound machine (GE Healthcare). To achieve a realistic focus depth in the tendon samples, an acoustic stand-off pad was placed between the transducer and the tendon and covered with ultrasound gel. Longitudinal images of the PVA phantom or tendons were recorded. Two frame rates were evaluated, 39.4 Hz with center frequency 13 MHz and 78.6 Hz with center frequency 10 MHz. One focus point at a depth of 3 cm was chosen.

For the examination of the surgically repaired and uninjured tendons in study III, a Vivid 7 ultrasound machine with an M12L linear array transducer (GE Healthcare) was used. The transducer was hand-held over the tendon during motion. Longitudinal images were then recorded during Thompson's squeeze test and active dorsiflexion using center frequency 14 MHz, frame rate 71.2 Hz and focus depth 3.5 cm. The same ultrasound system was used in the evaluation set-up in the first part of the same study. The transducer was mounted in a holder so that longitudinal images of the porcine flexor tendon with the inserted aluminum platelet could be obtained (14MHz, 65.3 FPS, depth 4 cm,).

In study IV a portable ultrasound system was required, so a Vivid-q ultrasound machine with a 9L linear array transducer (GE healthcare) was used. For ultrasound imaging of the Achilles tendon during walking, the transducer could not be hand-held. It proved to be a challenge to hold the transducer in place during walking and running and to avoid air to pass in between the transducer and the skin. Testing was done with attachments to the AFO and different types of holders. Finally a solution with a custom made foam plastic holder taped over the tendon and an acoustic standoff pad was found (Figure 9), and good quality long-axis images could be obtained (10 MHz, 40 FPS, depth 3 cm).

3.3.4 Speckle tracking motion estimation

Two different speckle tracking algorithms were used in this thesis, one commercially available algorithm and one in-house developed.

3.3.4.1 Commercial speckle tracking algorithm

Initial testing of three commercial speckle tracking algorithms on the tendon phantom described in 3.2.1 resulted in the choice of EchoPAC 110.1.2, 2D strain (GE Healthcare). Specifications regarding similarity measure, kernel size, kernel overlap and search areas for this algorithm were not known and could not be adjusted. The algorithm estimated strain within a chosen ROI as an average based on the motion estimates between kernels within that region. Two sizes of ROIs (11 mm and 22 mm) were evaluated. The ROIs were placed in the ultrasound sequences of the PVA phantom or tendon sample along the border facing the ultrasound transducer. The default settings for assessment of tracking quality, drift compensation and temporal and spatial smoothing were used. Strain data were then saved as text files. Mean strain curves for ten motion cycles and root mean square error (RMSE) between estimated strain and reference strain were calculated using Matlab. Peak strain was identified on all strain curves and compared to reference peak strain. The mean and SD of absolute errors was calculated for ten trials for the PVA phantom and tendon samples respectively using Excel (2013, Microsoft Corp., Redmond, USA).

3.3.4.2 In-house speckle tracking algorithm

The in-house speckle tracking algorithm used in study III and IV was originally developed for estimation of arterial wall strain [60]. The algorithm is written in Matlab and applied to B-mode ultrasound images and is based on block-matching of kernels as previously described. The similarity measure used is normalized cross correlation. It was adjusted regarding kernel size, shape and overlap to suit conditions expected in the Achilles tendon and several different settings were tested using the experimental set up descried in 3.2.1. A kernel size of 52λ (laterally) x 25λ (axially) and 80% kernel overlap was chosen and used in study III and IV.

For evaluation of the in-house algorithm it was applied to ultrasound acquisitions of the porcine tendons with inserted aluminum platelets described in 3.3.2 (study III). A five mm ROI was placed in the image superficial to the aluminum platelet and displacement was estimated. This was repeated for five trials for 5, 10 and 15 mm displacement at 5, 10 and 15 mm/s. Peak displacement estimated by speckle tracking was then compared to peak displacement found by manual tracking and mean, SD and coefficient of variation (SD/mean) of the absolute errors were calculated using Excel. Estimated peak displacement was plotted against reference peak displacement for all trails, a line was fitted to the plot and the Pearson coefficient of correlation was calculated using Origin 9.1.

To examine motion patterns in the surgically repaired and uninjured Achilles tendons a 20 mm ROI was used (study III). It was first placed in the superficial and then in the deep half of

the tendon. Displacement curves were plotted for all trials and peak superficial and deep displacement were identified and averaged for all trials and patients. Differential displacement was calculated as the difference between deep and superficial peak displacement.

For examination of motion patterns in the Achilles tendon during walking with different designs of AFO (study IV), the same tens steps that were chosen for EMG analysis were examined. A 25 mm ROI covering the full thickness of the tendon was used. An alteration was made to the algorithm so that it automatically divided the ROI in three parts and presented average displacement in superficial, middle and deep layers of the tendon. Superficial and deep displacement curves were interpolated and averaged for ten steps for all participants and walking conditions respectively. Peak superficial and deep displacement was identified for all steps. Differential displacement was calculated as the difference in peak deep and superficial displacements.

3.3.5 Plantar force measurement

In study I a 10 m force platform (Raute Corp, Finland), with two sections which could register right and left steps separately was used. GRF for the right foot were analyzed and used for identification of step cycles and stance phases for analysis of Achilles tendon force and EMG data. Mean GRF curves for one participant were presented in study I, Fig 2 [33].

3.3.6 Plantar pressure measurement

To investigate how plantar pressure is affected by different designs of AFO a plantar pressure insole system (Pedar-xf-16/R system, Novel GmbH, Munich, Germany) was used. This system has 99 sensors on each insole. Each participant was fitted with a pair of insoles which were held in place by compressive stockings and worn inside the AFO or running shoes. For the barefoot condition only the plantar pressure insole inside a compressive stocking were worn. Between each change in walking condition the unloaded pressure of the insoles was set to zero by lifting each foot in turn. Data was sampled at 100 Hz and sent to PC via Bluetooth® and exported as asc-files to Matlab. Heel strike times were identified in the plantar pressure data and used for determination of the beginning and end of each step. The foot was divided into three regions forefoot (distal 40%), midfoot (middle 30%) and rearfoot (proximal 30%) [8]. Forefoot and rearfoot pressure were then calculated as the average pressure of the sensors within each region. Peak pressure was identified for the same ten steps used for analysis of EMG and Achilles tendon displacement, and normalized to mean peak pressure during barefoot walking for each participant. Mean and SD peak pressure was then calculated.

3.4 STATISTICAL METHODS

For evaluation of the commercial and in-house speckle tracking algorithms in study II and III estimated strain or displacement were compared to reference, and mean and SD of the absolute errors were calculated in Excel. In study II RMSE for strain estimation for two

different frame rates and ROI sizes were compared using paired t-tests in Matlab. In study III the Pearson coefficient of correlation between estimated and reference peak displacement was found using Origin 9.1.

For comparison of displacement patterns between surgically repaired and uninjured tendons mean and SD of peak superficial and deep displacement were calculated. Peak superficial displacement was compared to peak deep displacement in individually matched couples using a paired t-test in Matlab. This was repeated for the comparison of differential displacement between surgically repaired and uninjured tendons.

In study I and IV comparisons were made between several walking conditions. In study I a repeated measures analysis of variance (ANOVA) using SAS (9.1, SAS Institute Inc., Cary, USA) was performed to find any statistical differences in Achilles tendon peak force, Achilles tendon force rate and EMG activity between AFO settings. The Tukey post hoc test was used to make pairwise comparisons of walking condition means. In study IV, SPSS (Statistics 24, IBM, Armonk, USA) was used to perform a repeated measures ANOVA to establish any differences in superficial displacement, deep displacement, differential displacement, EMG activity, forefoot pressure and rearfoot pressure between barefoot walking or any of the settings of each AFO design. Differential displacement and EMG activity of the different AFO designs were compared to each other and to barefoot walking, firstly for the conditions with least dorsiflexion limitation (rigid AFO 0 wedges, adjustable AFO 10° dorsiflexion and dorsal brace 0 wedges) and secondly for the conditions with most dorsiflexion limitation (rigid AFO 3 wedges and adjustable AFO 30° plantarflexion). The dorsal brace was not included in the second comparison as it did not achieve the same degree of plantarflexion. Mauchly's test of Sphericity was used to test the assumption of sphericity, and when violated the Greenhouse-Geisser correction was used. The Bonferroni correction was used to make pairwise comparisons of condition means. EMG activity in study I and plantar pressure in study IV were normalized to the mean during barefoot walking which was set to 100%. For comparisons between AFO conditions and barefoot walking the 95% confidence intervals (CI) of the condition means were calculated, and if the CI did not include 100% the difference was considered statistically significant.

4 RESULTS

4.1 EVALUATION OF DISPLACEMENT AND STRAIN ESIMATION IN TENDON TISSUE (STUDY II AND III)

Mean peak estimated strain, mean peak reference strain and RMSE between estimated strain and reference strain for the commercial speckle tracking algorithm are shown in Table 2. RMSE for estimation of strain in the tendon samples was significantly lower when using frame rate 39.4 Hz as compared to 78.6 Hz. In two of the tendon samples, RMSE were significantly lower when using the larger ROI (22 mm vs 11 mm).

	Estimated peak strain mean ± SD (%)	**Reference peak strain mean ± SD (%)**	**RMSE (%)**
PVA phantom	4.32 ± 0.05	4.07 ± 0.00	0.21 ± 0.08
Porcine tendon 1	6.01 ± 0.59	4.41 ± 0.00	1.36 ± 0.40
Porcine tendon 2	18.96 ± 3.95	4.12 ± 0.02	10.64 ± 3.40
Porcine tendon 3*	4.20 ± 1.33	4.16 ± 0.01	1.85 ± 0.76
Human allograft	3.77 ± 0.89	4.19 ± 0.01	1.19 ± 0.12

Table 2. *Evaluation of the commercial speckle tracking algorithm for estimation of strain. Mean and standard deviation of estimated peak strain (%), reference peak strain (%) and root mean square error (RMSE) between estimated strain and reference strain (in % strain) for 22 mm ROI and 39.4 FPS). * n=8*

Correlations between tendon displacement estimated by the in-house speckle tracking algorithm and reference displacement found by manual tracking are shown in Figure 11. The speckle tracking algorithm constantly underestimated tendon displacement for all conditions. The materials testing machine was programmed to displace the tendon 5 mm, 10 mm and 15 mm at 5 mm/s, 10 mm/s and 15 mm/s and these settings resulted in displacements of 4.1 mm, 8.4 mm and 12.1 mm and velocities of 4.1 mm/s, 7.7 mm/s and 11.5 mm/s respectively, as found by manual tracking. For 5 mm and 10 mm displacement at 5mm/s and 10 mm/s respectively, the coefficients of variation were between 1.4 and 11.7 for the two porcine tendons.

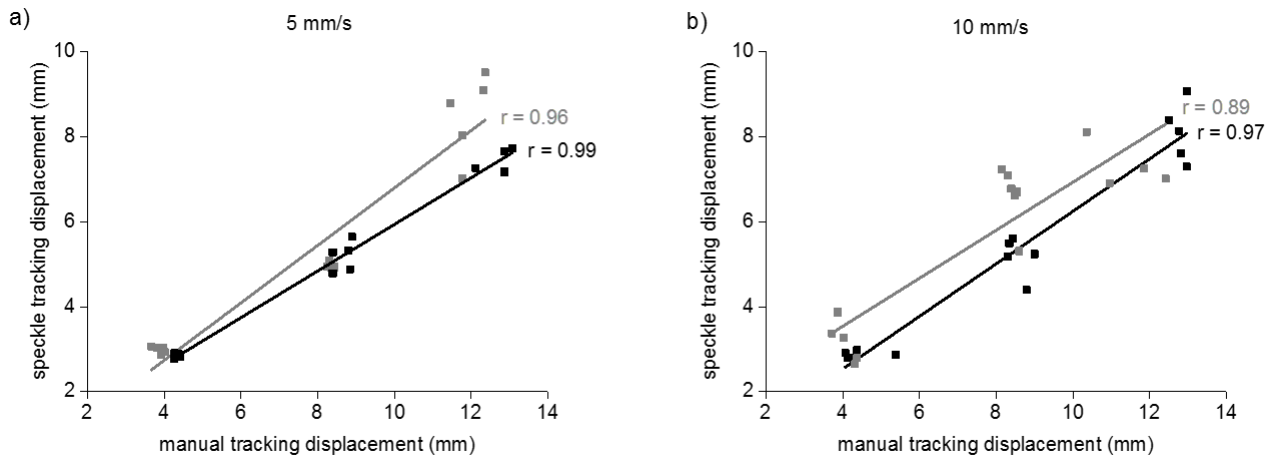

Figure 11. *Correlation between peak displacement (mm) as estimated by the in-house speckle tracking algorithm and reference displacement at* ***a*** *5 mm/s and* ***b*** *10 mm/s for porcine tendon 1 (black) and porcine tendon 2 (grey). r = Pearson coefficient of correlation, p< 0.01 for all correlations. (Reprinted from study III [32], https://doi-org.proxy.kib.ki.se/10.1007/s00167-016-4394-5)*

4.2 LOAD AND DEFORMATION IN THE ACHILLES TENDON (STUDY I, III AND IV)

Achilles tendon mean peak force and mean rate of force development during walking in an adjustable AFO (study I) are shown in Table 3. Achilles tendon force showed a tendency to increase as restriction in dorsiflexion increased. Peak Achilles tendon force was significantly ($p<0.01$) smaller during barefoot walking than when using an adjustable AFO set at 20° plantarflexion. There were no significant differences for rate of Achilles tendon force development between any of the conditions.

	barefoot	**10° dorsiflexion**	**10° plantarflexion**	**20° plantarflexion**
AT peak force (*bw) mean ± SD	2.1 ± 0.7	2.6 ± 0.6	2.6 ± 1.0	3.1 ± 1.1
AT force rate (N/s) mean ± SD	2799 ± 1325	2580 ± 1218	1999 ± 803	2192 ± 1175

Table 3. *Mean ± SD Achilles tendon (AT) peak force normalized to bodyweight and AT rate of force development during walking barefoot and in an adjustable AFO. 10° dorsiflexion = dorsiflexion limited to 10° dorsiflexion with unrestricted plantarflexion, 10° plantarflexion = dorsiflexion limited to 10° plantarflexion with unrestricted plantarflexion, 20° plantarflexion = locked at 20°, *bw = normalized to bodyweight. (Data adapted from study I [33])*

Mean displacement curves for surgically repaired and uninjured tendons during Thompsons's squeeze test and active dorsiflexion are shown in Figure 12. The difference in peak displacement between superficial and deep tendon layers was significantly ($p<0.01$) higher in the uninjured tendons compared to the surgically repaired tendons. Displacement in the deep tendon layers was significantly ($p<0.01$) higher than in the superficial layers for both surgically repaired and uninjured tendon during active dorsiflexion, but only for the uninjured tendons during Thompson's squeeze test.

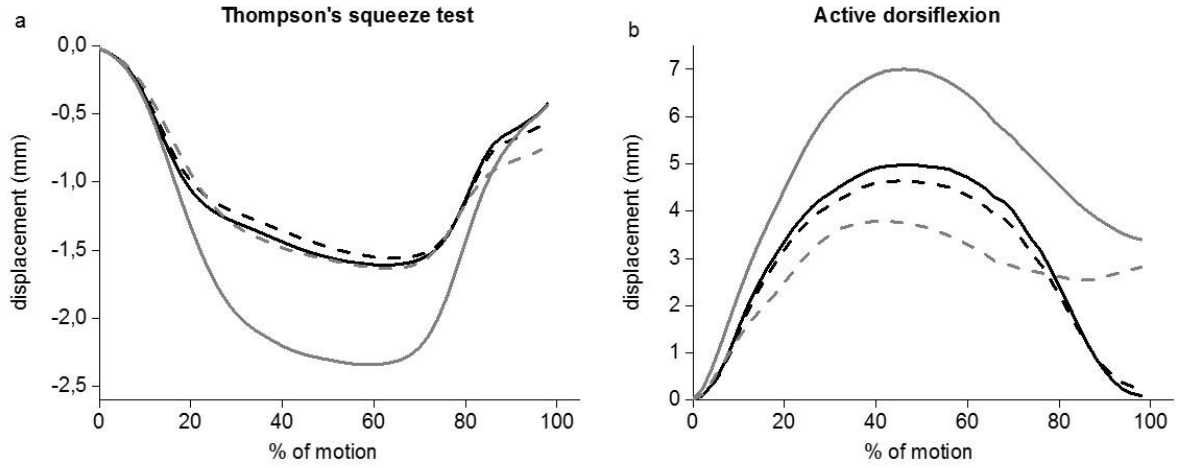

Figure 12. *Mean displacement in the superficial (dashed) and deep (solid) layers of surgically repaired (black) and uninjured (grey) Achilles tendons for 11 patients during* ***a.*** *Thompson's squeeze test and* ***b.*** *active dorsiflexion. (Reprinted from study III [32], https://doi-org.proxy.kib.ki.se/10.1007/s00167-016-4394-5)*

Mean Achilles tendon displacement curves for barefoot walking and walking in three different designs of AFO are shown in Figure 13. Mean peak displacement in the deep tendon layers was significantly larger ($p<0.01$) than in the superficial layers for all walking conditions. Difference in superficial and deep displacement was significantly reduced ($p<0.05$) in the rigid AFO as the number of wedges increased from zero to three and in the adjustable AFO as restriction in dorsiflexion increased from 10° dorsiflexion to 30° plantarflexion. There were no significant differences in differential displacement between the rigid AFO 0 wedges, the adjustable AFO 10° dorsiflexion and the dorsal brace 0 wedges or between the rigid AFO 3 wedges and the adjustable AFO 30° plantarflexion.

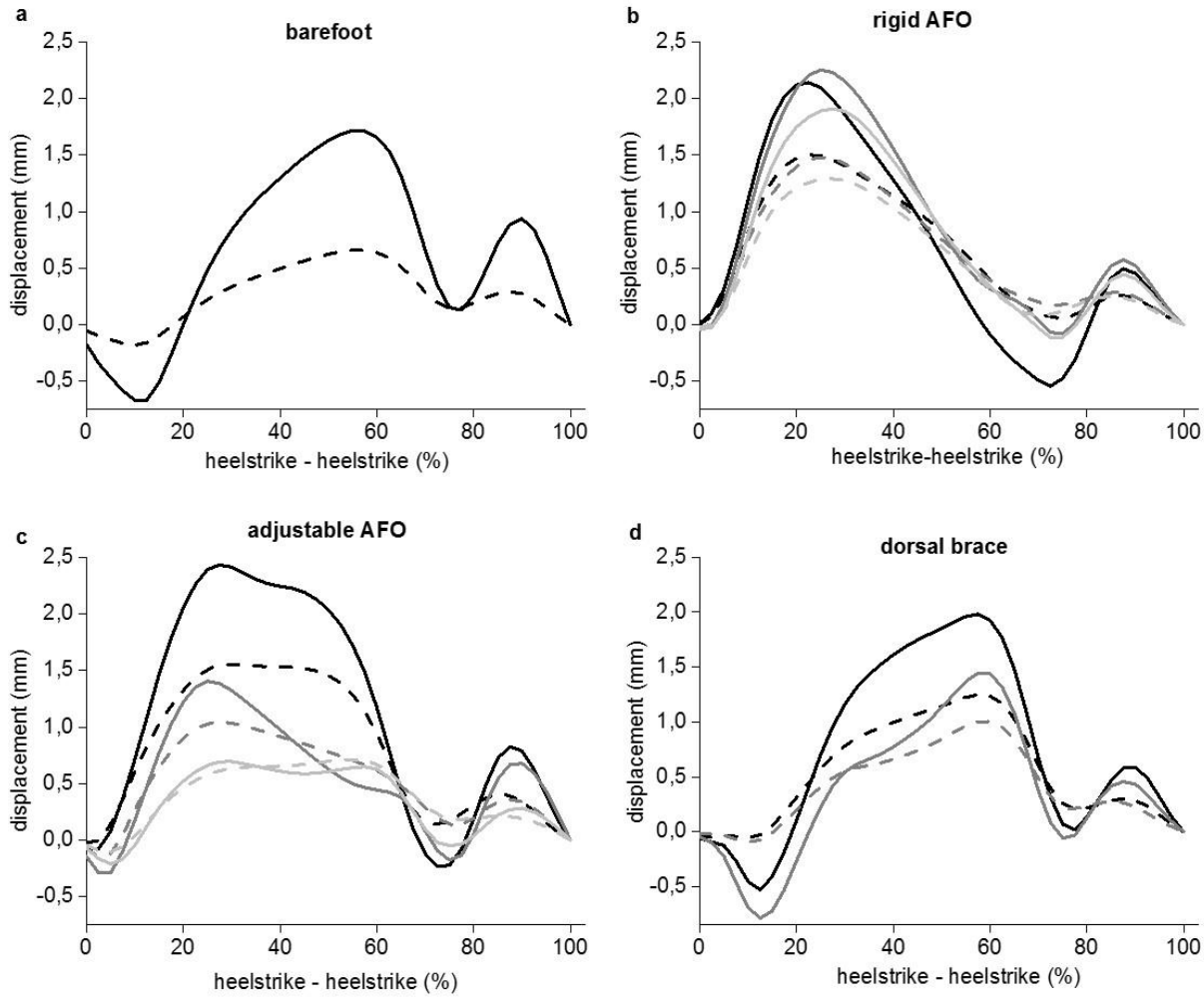

Figure 13. *Mean displacement in the superficial (dashed) and deep (solid) layers of the Achilles tendon during walking on a treadmill at 2 km/h for 16 healthy participants under different conditions.* ***a.*** *barefoot walking* ***b.*** *rigid AFO with 0 wedges (black), 2 wedges (grey) and 3 wedges (light grey).* ***c.*** *adjustable AFO with ankle dorsiflexion limited to 10° dorsiflexion (black), 10° plantarflexion (grey) and 30° plantarflexion (light grey)* ***d.*** *dorsal brace with 0 wedges (black) and 1 wedge (grey).*

4.3 EMG OF LOWER LEG MUSCLES DURING USE OF AFO (STUDY I AND IV)

During use of the rigid AFO there was a decrease in medial and lateral gastrocnemius and soleus activity compared to barefoot walking ($p<0.05$), and activity was lowest when three wedges were used (Figures 14 and 15). There was no significant difference in tibialis anterior activity between barefoot walking and the rigid AFO with any number of wedges. In the adjustable AFO, soleus activity decreased as dorsiflexion was progressively limited and the decrease was significant ($p<0.05$ or 95% CI did not include 100%) when the AFO was set at plantarflexion beyond 10° (Figure 15). Medial gastrocnemius activity varied between settings so that is was lower for the settings limiting dorsiflexion to 10° dorsiflexion and 30° plantarflexion than for the setting limiting dorsiflexion to 10° plantarflexion (Figure 14).

Using the adjustable AFO, tibialis anterior activity was significantly higher ($p<0.05$ or 95% CI did not include 100%) when dorsiflexion was limited to 10° plantarflexion than for barefoot walking. When the dorsal brace was used, muscle activity in the medial gastrocnemius and soleus was reduced compared to barefoot walking but the addition of one 10 mm heel wedge did not significantly affect muscle activity (Figure 14 and 15). There was no significant difference in tibialis anterior activity between barefoot walking and any of the dorsal brace conditions.

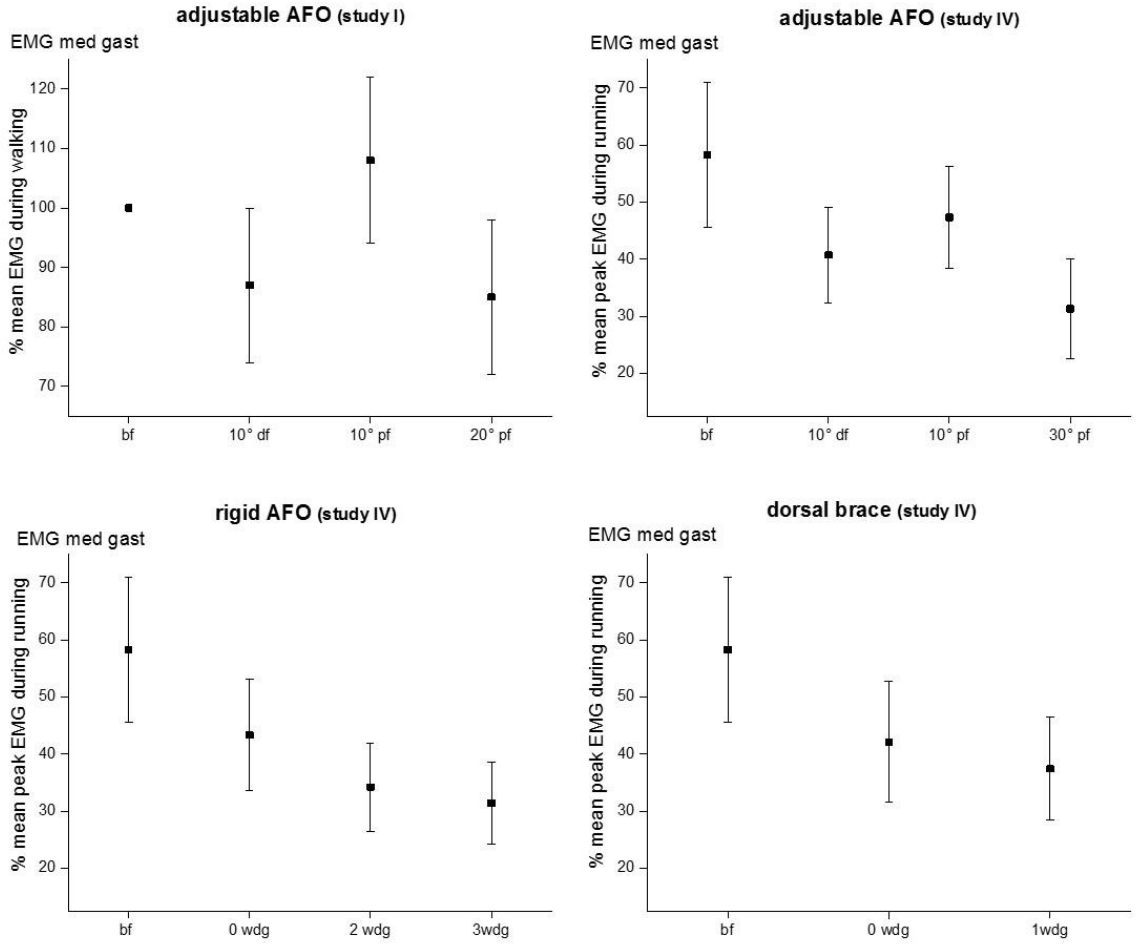

Figure 14. *Mean EMG activity in the medial gastrocnemius with 95% CI. For the adjustable AFO in study I EMG is expressed as a percentage of mean EMG during barefoot walking. For the adjustable AFO in study IV, the rigid AFO and the dorsal brace EMG is expressed as a percentage of mean EMG during running. bf = barefoot, df = dorsiflexion, pf = plantarflexion, wdg = wedge.*

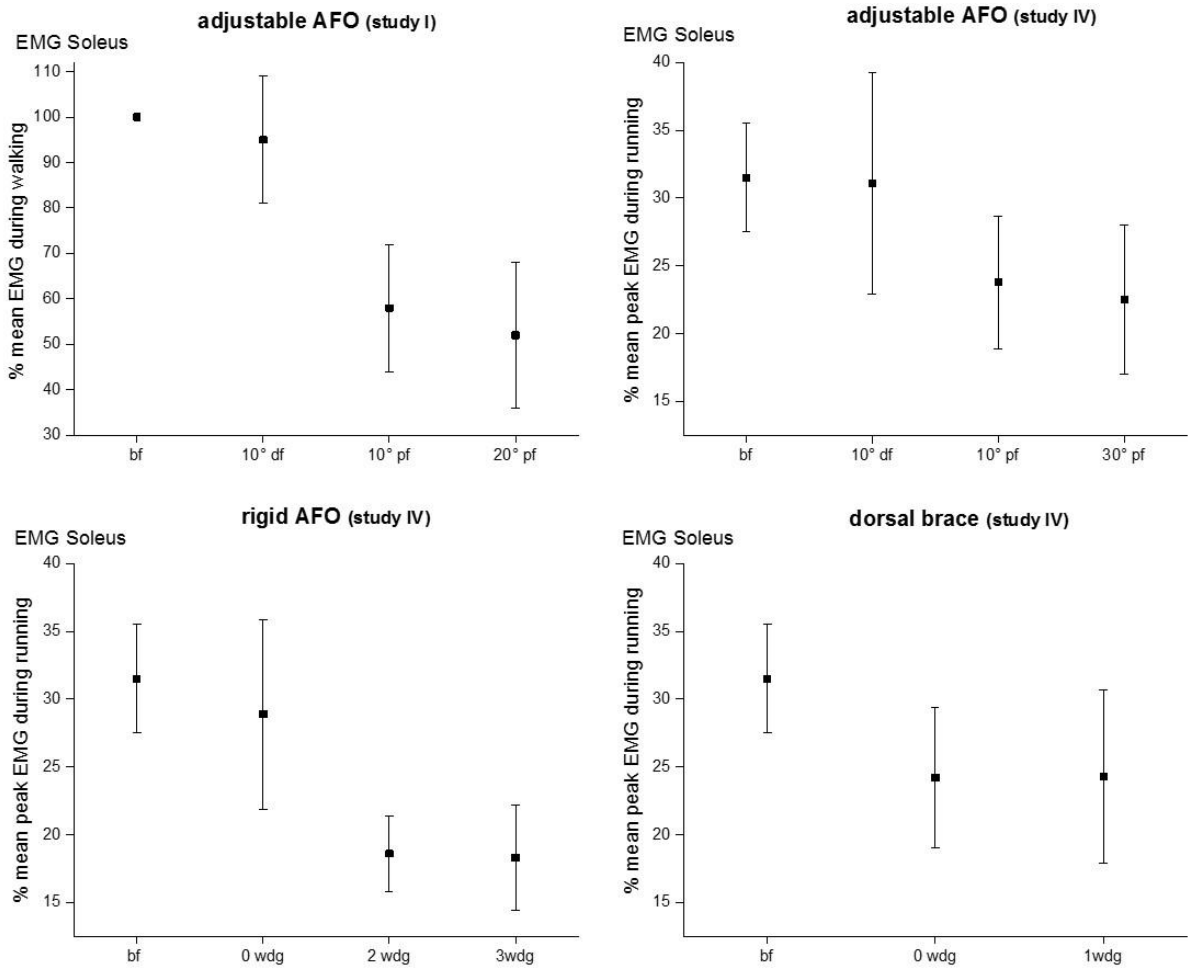

Figure 15. *Mean EMG activity in the soleus with 95 % CI. For the adjustable AFO in study I EMG is expressed as a percentage of mean EMG during barefoot walking and for the adjustable AFO in study IV, the rigid AFO and the dorsal brace EMG is expressed as a percentage of mean EMG during running. bf = barefoot, df = dorsiflexion, pf = plantarflexion, wdg = wedge.*

4.4 PLANTAR PRESSURE DURING USE OF AFO

Forefoot pressure was significantly reduced compared to barefoot walking (the 95% CI did not include 100%) for all the AFO designs. During use of the rigid AFO forefoot pressure was 48% (39-58) of barefoot pressure with zero wedges, 42% (31-52) with two wedges and 34% (24-43) with three wedges, which was a significant reduction with each extra wedge ($p<0.05$). When the adjustable AFO was used, forefoot pressure was significantly reduced ($p<0.05$) with each stepwise reduction in permitted dorsiflexion range of motion and was 69% (57-82) of barefoot pressure with a 10° dorsiflexion limit, 45% (33-57) with a 10° plantarflexion limit and 27% (17-36) with a 30° plantarflexion limit. For the dorsal brace forefoot pressure was 65% (53-77) of barefoot pressure with zero wedges and 72% (58-86) when one wedge was used.

5 DISCUSSION

5.1 ULTRASOUND SPECKLE TRACKING IN TENDONS

Ultrasound systems are commonly available for use in clinical practice and software for speckle tracking motion analysis is commonly included. It can be tempting to apply the software to ultrasound sequences for estimation of motion in any tissue. However, the commercially available speckle tracking algorithms are commonly developed and tested only for motion estimation in the myocardium and motion estimation in other types of tissue with different speckle pattern and different magnitude and velocity of displacement may require adjustments of the algorithm. In study II a commercial speckle tracking algorithm was assessed to determine if it would be feasible to use for strain estimation in tendon tissue. The algorithm performed well on the PVA phantom whereas a high variability in measurement errors was found in the tendon samples. As the dimensions and speed of motion of the PVA phantom and tendon samples were similar, the difference is probably explained by differences in speckle pattern and elastic properties. Speckles in the PVA phantom were small, distinct and evenly distributed and presumably easier to track. Inhomogeneity in elastic properties along the length of the tendon samples may have led to local variations in strain, which was probably avoided in the homogenous PVA phantom. The high variability in measurement errors in the tendon samples makes the results unpredictable. The commercially available speckle tracking algorithm evaluated in study II has previously been used to evaluate strain in the supraspinatus tendon during elevation of the arm and remarkable large variations in strain were reported [52]. Results indicate that the algorithm used was not suitable for motion estimation in tendons [92]. It is important to be aware of the limitations of speckle tracking software when interpreting results and study II has contributed to highlighting this issue.

The speckle tracking algorithm used for estimation of displacement in tendon tissue in studies III and IV was evaluated in study III. A high correlation was found between displacement estimated by speckle tracking and displacement estimated by manual tracking of an aluminum platelet in the tendon, but the speckle tracking algorithm was found to constantly underestimate displacement. Varying degrees of underestimation of displacement by speckle tracking in tendon tissue have been observed before. A commercial speckle tracking algorithm (Syngo VVI software, Siemens Medical Solutions Inc., Malvern, USA) was validated for measuring displacement in human flexor digitorum tendons and underestimation was found to be larger than for the in-house algorithm in study III [106]. Chernak et al also found high correlations between estimated displacement and reference displacement and a similar tendency for underestimation of displacement by speckle tracking as in study III [19]. Korstanje et al showed lower measurement errors for estimation of displacement [59]. The observed underestimation is likely due to momentary loss of tracking caused by tendon motion out of the ultrasound plane or difficulties in tracking the striated speckle pattern. For the magnitudes of tendon displacements and velocities seen during active dorsiflexion and Thompson's test in study III, the coefficient of variation of the measurement error was less

than 11.7%. During walking at 2 km/h the magnitudes of tendon displacements and velocities were smaller and the coefficient of variation of the measurement error was less than 2.7%. Measurement errors can be described in terms of both precision and variability. Measurement errors that have a low variability can be compensated for, whereas errors with high variability are more difficult to handle. When interpreting the results of studies III and IV the underestimation should be considered. In both studies displacement in different parts of the tendons could be distinguished with statistical significance which indicates that the method is applicable.

5.2 ALTERED PATTERNS OF DISPLACEMENT IN THE ACHILLES TENDON FOLLOWING INJURY

The non-uniform displacement pattern with larger displacement in deep compared to superficial tendon layers that was observed in the uninjured tendons, is similar to that described in previous studies [4,31,93]. In the surgically repaired tendons, displacement was more homogenous across the thickness of the tendon. It has been suggested that the non-uniform displacement pattern described in uninjured tendons reflects gliding between tendon fascicles [4,93]. Following rupture and scar tissue formation normal tendon morphology is altered, and the more uniform displacement pattern seen in the surgically repaired tendons in study III may be explained by a decreased ability of tendon fascicles to glide past each other. A similar decrease in the non-uniform displacement pattern of the Achilles tendon has also been observed in old compared to young adults during walking, and the difference was more pronounced at higher walking speeds (4.5 km/h) [31]. The more uniform tendon displacement patterns in old adults were correlated with reduction in plantarflexion moment, power and work during push off and are thought to be explained by increased collagen crosslinking with age [31]. Impaired fascicle gliding following rupture may have negative effects on the modulation of the actions of the different muscles of the triceps surae and may impair optimal force transmission at different knee and ankle joint angles. After an Achilles tendon rupture long term reduction in plantarflexion function compared to the uninjured leg is commonly seen [76,78,104], and the alterations in tendon deformation patterns observed in the surgically repaired tendons in study III may in part explain this. In animal studies loading of growing and healing tendons resulted in earlier formation of tendon tissue with thicker, better organized collagen oriented in line with tendon stress [17,50]. In patients with surgically treated Achilles tendon ruptures, active loaded plantarflexion exercises starting two weeks after injury resulted in higher tendon elastic modulus [87]. There is little knowledge of how loading of healing human Achilles tendons affects tendon morphology, but it can be speculated that repair tissue with better organized parallel collagen fibers may have better gliding properties which may in turn improve force transmission.

5.3 EFFECTS OF THE ANKLE FOOT ORTHOSES

5.3.1 Tendon load and deformation

For the adjustable AFO used in study I, force in the Achilles tendon was significantly higher when dorsiflexion was limited to 20° plantarflexion than during barefoot walking. This was an unexpected finding at the time as it had previously been shown that muscle activity in the gastrocnemius and soleus, which was also related to plantarflexion torque, decreased when the rigid AFO design was used with increasing number of wedges [1]. A possible explanation is that when the adjustable AFO design is set in plantarflexion it lacks support under the heel and the user is forced to support on the toes which makes it difficult to achieve a relaxed gait pattern. The plantarflexed setting is commonly used early in Achilles tendon rupture treatment protocols to adapt tendon ends, and at this stage patients are often instructed to use crutches. If this AFO design is to be used in more active treatment protocols with early full weight bearing, the risk of tendon forces which are higher than during barefoot walking should be considered for the most plantarflexed positions.

To our knowledge study IV is the first study in which deformation patterns and muscle activity have been studied simultaneously in AFO and compared between different AFO designs. A non-uniform displacement pattern with larger displacement in deep tendon layers compared to superficial layers was present for all AFO conditions. No significant differences in differential displacement were seen between the AFO designs despite their differences. Since force in the Achilles tendon had been shown to increase with increasing limitation in dorsiflexion for the adjustable AFO in study I, while plantarflexion torque as estimated through EMG had previously been shown to decrease with increasing dorsiflexion limitation in a rigid AFO [1], some difference in tendon deformation pattern was expected between these designs. Instead the degree of limitation in dorsiflexion within each AFO design seemed to influence displacement patterns more. When the rigid or the adjustable AFO were used, displacement patterns in the tendon became more uniform as restriction in dorsiflexion increased. In rat models of Achilles tendon ruptures it has been shown that loading on the injured limb is beneficial to healing [2,3,17,25], but which type of loading provides the best stimulus is not known [2]. However, from rat models it appears that full time free and gradually increasing weigtbearing is more effective in stimulating healing than unloading with intermittent episodes of running [2]. It is not clear how these results translate into human Achilles tendons, but it may indicate that loading which mimics barefoot walking is a good stimulus for healing. The results of study IV show that the AFO settings with least limitation in dorsiflexion resulted in non-uniform tendon deformation patterns most resembling those during barefoot walking. A limitation of study IV is that it was conducted on healthy participants who were not limited by pain or caution when loading their braced leg, and deformation patterns in injured tendons may be different.

5.3.2 Muscle activity

Muscle activity in medial and lateral gastrocnemius and soleus decreased compared to barefoot walking when the rigid AFO was used, and muscle activity continued to decrease with the addition of wedges. This is in agreement with previous results concerning this AFO design [1,46]. For the adjustable AFO investigated in study I and IV, soleus muscle activity decreased as dorsiflexion became gradually more restricted, in a manner similar to that in the rigid AFO with wedges. Muscle activity in the gastrocnemius showed a different pattern, where activity at the setting restricting dorsiflexion to 10° plantarflexion was higher than when dorsiflexion was restricted to 10° dorsiflexion. As mentioned previously this AFO lacks support under the heel when set in plantarflexed positions and participants supported on their toes and flexed the knee to varying degrees to avoid limping. Bending the knee is likely to affect EMG in the gastrocnemius due to the change in muscle length, but have less effect on the soleus. When using the adjustable AFO, muscle activity in tibialis anterior increased compared to barefoot walking when dorsiflexion was limited to 10° plantarflexion (study I and IV) and in study IV activity continued to increase with further dorsiflexion limitation. This may have been due to an increased effort to dorsiflex the foot during swing phase to avoid tripping and may lead to increased passive pull on the Achilles tendon. The main function of the dorsal brace was to restrict dorsiflexion to neutral and it did not offer the same degree of ankle support as the other AFO designs, but still gastrocnemius and soleus EMG activity was reduced compared to barefoot walking. For all the AFO designs EMG activity in the triceps surae was reduced as dorsiflexion was limited and the muscles shortened. In animal models it has been shown that calf muscles undergo more atrophy if they are immobilized in shortened positions than if they are immobilized in neutral or lengthened positions [16,80,91]. Limb immobilization leads to loss of muscle mass and strength and to a reduction in muscle protein synthesis rate [23,102]. It has been shown that these effects can be partly counteracted if electrical activity is maintained by neuromuscular electrical stimulation [23], which may indicate that a maintained EMG activity is positive for prevention of atrophy. In study IV it was shown that the AFO designs and settings which permitted more dorsiflexion resulted in less reduction in soleus and gastrocnemius activity and less triceps surae muscle shortening which is likely to be beneficial in preventing muscle atrophy. Immobilization with a dorsal brace with neutral ankle angle and weight bearing as tolerated was compared to a below the knee cast in equinus with no weight bearing following surgical repair of the Achilles tendon, and resulted in significantly less calf muscle atrophy [67].

5.3.3 Plantar pressure

Forefoot pressure was reduced compared to barefoot walking for all AFO conditions and in the rigid and adjustable AFO the reduction in forefoot pressure became more pronounced as limitation of dorsiflexion increased. Forefoot pressure has previously been shown to correlate to the degree of dorsiflexion allowed within an AFO [50]. During walking the forefoot is used for push-off against the ground and therefore forefoot pressure has been suggested as an important outcome to evaluate regarding Achilles tendon function [50]. Although forefoot

pressure can be expected to be affected by a number of factors, it was noted that it showed a similar tendency to decrease with increasing dorsiflexion limitation as non-uniform displacement in the Achilles tendon and muscle activity in the triceps surae.

5.3.4 AFO settings

AFO designs and settings which permitted more dorsiflexion resulted in a more non-uniform displacement pattern within the Achilles tendon and less reduction in gastrocnemius and soleus muscle activity, which may be beneficial to stimulate tendon healing and prevent muscle atrophy. However, to protect the healing tendon from elongation following surgical or non-surgical treatment of an Achilles tendon rupture, it is common to place the ankle in plantarflexion in a cast or AFO which is then gradually reduced to neutral [70,76,78,88,101,104]. There are a few studies of surgical treatment of Achilles tendon ruptures where the ankle was immobilized in neutral and weight bearing was allowed early in the treatment protocol. A dorsal brace permitting free plantarflexion and dorsiflexion to neutral applied either the day after surgery [48] or after two weeks [67] and full weight bearing allowed after 2-3 weeks was compared to cast treatment. There were no differences in re-rupture rate between the groups in any of the studies, and less decrease in calf muscle circumference [67], less reduction in calf muscle strength and no increase in tendon elongation [47,48] in the braced group. The adjustable AFO design set to limit dorsiflexion to neutral with unlimited plantarflexion applied two weeks postoperatively, has been compared to cast treatment and there was no difference in re-rupture rate or tendon elongation and patients in the AFO group regained ankle range of motion and returned to work earlier [74]. The above studies [47,48,67,74] indicate that for surgically treated Achilles tendon ruptures it is safe to put the ankle in neutral position early, whereas evidence is lacking for non-surgically treated ruptures.

5.4 METHODOLOGICAL CONSIDERATIONS

5.4.1 Optic fiber measurements (study I)

There are some limitations to the fiber optic force sensor technique used in study I. Calibrations of the optic fiber output signal to plantarflexion moment were made under static conditions, whereas the experiments were dynamic. To decrease errors due to mismatch between calibration and experimental conditions it has been recommended to use dynamic calibration [28]. However as plantarflexion and Achilles tendon moment arms about the ankle vary during ankle motion, dynamic force calculations are difficult and there are no other feasible alternatives for dynamic calibration for human in-vivo studies. Cable migration is another known source of error with this technique and was controlled for in study I by visual inspection [28]. Measurement artifacts caused by movement of the skin at the fiber insertion site may also affect results, but reports of the magnitude of these errors vary greatly [27,29]. Finni et al investigated this by pulling the skin over the Achilles tendon near the inserted optic fiber and report errors in the magnitude of 2% of peak forces recorded during walking [29]. In an experimental set up with a gait simulator using cadaver feet, force

measurement errors were found to vary between 24-81% of peak forces when the skin was intact and between 10-33% of peak forces after the skin had been removed [27]. However, skin properties of a cadaver foot may not be directly comparable to the in-vivo situation. Achilles tendon forces previously measured using the optic fiber technique during walking correspond well to those measured using the buckle transducer [30]. The above limitations should be kept in mind when interpreting the results.

5.4.2 Plantar pressure measurements (study IV)

Insoles for plantar pressure measurement can only measure force normal to the sensors, whereas medio-lateral and anterio-posterior forces cannot be measured. If the measurement insole is placed on an uneven or inclined surface only the force component normal to the surface will be measured, and there is risk for an underestimation of the vertical force [95]. In study IV plantar pressures were measured at different angles of plantarflexion. In the rigid AFO and dorsal brace plantarflexion was achieved with heel wedges. In these AFO the inclination of the measurement insole was most pronounced under the rear- and midfoot, whereas the forefoot was flat. In the adjustable AFO there was an inclination of the entire measurement insole in the plantarflexed positions. This is a potential source of measurement error. It has also been shown that the stiffness of the surface on which the sensor is placed may affect measurements, which should be considered when comparisons are made between different footwear [95]. The inner surface of the AFO and the running shoes used with the dorsal brace had similar stiffness. During the barefoot condition, participants walked directly on the treadmill which had a stiffer surface and this may have introduced errors when comparing AFO conditions to barefoot walking.

5.5 FUTURE PERSPECTIVES

In recent years ultrasound speckle tracking has been used to demonstrate non-uniform displacement patterns in uninjured Achilles tendons and that these patterns are altered by age and following injury. Further research is needed to explain the cause and function of these non-uniform displacement patterns and how disturbed patterns affect tendon function. Understanding of how these properties can be affected in healing tendons may be useful in designing treatment protocols. With improvements in ultrasound tracking techniques it is becoming possible to accurately estimate strain in tendon tissue which is likely to be a more important factor in understanding Achilles tendon function. Ultrasound based measurements for study of tendon biomechanics is a promising field as ultrasound is non-invasive and radiation free. Ultrasound equipment is becoming more portable and less expensive which makes it more readily available close to patients and athletes in clinical practice. With the development of 3D ultrasound the problem of out of plane motion is likely to be solved and measurement accuracy of tracking algorithms can be expected to improve. Commercial algorithms developed for tracking of tendon tissue will advance the field even further as the technique will be available to all.

6 CONCLUSIONS

The general aims of this thesis were to improve understanding of how injury and use of AFO affect load and deformation within the Achilles tendon and to adapt and evaluate an ultrasound based method for studying the biomechanics of the Achilles tendon during motion.

- During walking in an adjustable AFO with full weight bearing, Achilles tendon force increased compared to barefoot walking when dorsiflexion was restricted and the ankle was plantarflexed, despite reduction in soleus EMG activity (study I). These results raised the question if different designs of ankle foot orthoses affect the Achilles tendon in different ways. Experience with the invasive optic fiber technique lead to the choice of developing a non-invasive ultrasound based technique to study Achilles tendon biomechanics which would be more applicable on injured tendons.
- High variability in strain estimation errors were found when a commercial ultrasound based speckle tracking algorithm developed for motion estimation in cardiac muscle was evaluated for estimation of strain in tendon tissue (study II). These results highlight the need for speckle tracking software to be evaluated before it is applied to new tissues and that it is important to be aware of its limitations when interpreting results.
- An in-house developed speckle tracking algorithm for estimation of displacement in tendon tissue was shown to underestimate tendon displacement, but for the magnitude and velocity of displacement relevant during range of motion exercise and walking, low coefficients of variation were found (study III). Displacement in different parts of the tendons could be distinguished with statistical significance and it was concluded that the method is clinically applicable.
- A more uniform displacement pattern was observed in previously ruptured and surgically repaired Achilles tendons compared to the non-uniform displacement pattern observed in uninjured tendons (study III). The altered displacement pattern is interpreted as a reduction in gliding between tendon fascicles which is proposed as a contributing explanation of reduced calf musle function.
- The degree of dorsiflexion limitation within an AFO had greater effects on tendon displacement patterns and triceps surae muscle activity than differences in AFO design (study IV). AFO settings with least limitation in dorsiflexion resulted in tendon deformation patterns and triceps surae muscle activity most resembling those during barefoot walking.

7 ACKNOWLEDGEMENTS

I wish to express my gratitude to all those who have contributed to this thesis, and in particular to:

Toni Arndt, principal supervisor. Thank you for guiding me into the field of biomechanical research and for sharing your enthusiasm for trying new techniques and your belief that problems are for solving.

Tomas Movin, co-supervisor, for the first introduction into research and for your encouragement over the years.

Birgitta Janerot Sjöberg, co-supervisor, for introducing me to imaging technology and for your support and good advice.

Mattias Mårtensson, co-author. Thank you for an invaluable cooperation with experimental design, data collection, statistical analysis and manuscript writing and above all the fruitful discussions and good laughs.

Matilda Larsson, co-author. Thank you for sharing your speckle tracking algorithm, for explaining the mysteries of ultrasound imaging and speckle tracking and for your feed-back on the manuscripts and thesis.

Ann-Sophie Cissé, co-author and colleague for a good cooperation and all the good times during residency.

Paavo Komi, for providing the facilities for the experiments of the first study and for introducing me to optic fiber force measurements.

Olga Tarassova, for your help and problem solving in the biomechanical laboratory.

Johanna Ungerstedt, personal researcher and friend. Thank you for sharing your never ending energy and for your help with my half time seminar and thesis writing.

Li Felländer-Tsai, head of unit, for good advice and for your support of this thesis project.

Paul Gerdhem, former director of doctoral studies, for answering all the big and small questions regarding a thesis project.

Hans Berg, colleague, for your advice about my research project and for stimulating biomechanical discussions in the coffee room.

Harald Brismar, colleague, for all your good advice and support in research and clinical work.

Margareta Hedström, Anders Herrlin, Kjell Keisu, Nicolas Martinez and **Ricard Miedel**, my colleagues at the arthroplasty surgery unit for your support.

Anna Andersen, my great friend and support in all aspects of life.

Anna Grauers, for being a good friend and colleague during residency and my long way towards finishing my thesis project.

Rusana Bark and **Neda Rajamand Ekberg** for being good friends and making research sound so easy.

Erik Almgren and **Tomas Andersen** for your help with programming.

My parents **Marianne** and **Bo-Göran Ryberg** and my parents in law **Anette** and **Jan Fröberg** for all the help with the children. Without your help, writing this thesis would never have been possible.

My husband, **Tommy Fröberg**, thank you.

8 REFERENCES

1. Akizuki KH, Gartman EJ, Nisonson B, Ben-Avi S, McHugh MP (2001) The relative stress on the Achilles tendon during ambulation in an ankle immobiliser: implications for rehabilitation after Achilles tendon repair. British journal of sports medicine 35 (5):329-333; discussion 333-324

2. Andersson T, Eliasson P, Aspenberg P (2009) Tissue memory in healing tendons: short loading episodes stimulate healing. Journal of applied physiology (Bethesda, Md : 1985) 107 (2):417-421. doi:10.1152/japplphysiol.00414.2009

3. Andersson T, Eliasson P, Hammerman M, Sandberg O, Aspenberg P (2012) Low-level mechanical stimulation is sufficient to improve tendon healing in rats. Journal of applied physiology (Bethesda, Md : 1985) 113 (9):1398-1402. doi:10.1152/japplphysiol.00491.2012

4. Arndt A, Bengtsson AS, Peolsson M, Thorstensson A, Movin T (2012) Non-uniform displacement within the Achilles tendon during passive ankle joint motion. Knee surgery, sports traumatology, arthroscopy : official journal of the ESSKA 20 (9):1868-1874. doi:10.1007/s00167-011-1801-9

5. Arndt A, Bruggemann GP, Koebke J, Segesser B (1999) Asymmetrical loading of the human triceps surae: I. Mediolateral force differences in the Achilles tendon. Foot & ankle international 20 (7):444-449

6. Arndt A, Notermans HP, Koebke J, Bruggemann GP (1997) Zur Fasertextur der menschlichen Achillessehne - Eine Analyse durch Mazeration Der Präparator 43 (3):63-70

7. Arndt AN, Komi PV, Bruggemann GP, Lukkariniemi J (1998) Individual muscle contributions to the in vivo achilles tendon force. Clinical biomechanics (Bristol, Avon) 13 (7):532-541

8. Barnett S (1998) International protocol guidelines for plantar pressure measurement. The Diabetic Foot 1 (4):137-140

9. Benjamin M, Kaiser E, Milz S (2008) Structure-function relationships in tendons: a review. Journal of anatomy 212 (3):211-228. doi:10.1111/j.1469-7580.2008.00864.x

10. Berne RM, Levy MN (1993) Physiology. 3 rd edn. Mosby Year Book Inc, St Louis, Missouri, USA

11. Bleakney RR, Tallon C, Wong JK, Lim KP, Maffulli N (2002) Long-term ultrasonographic features of the Achilles tendon after rupture. Clinical journal of sport medicine : official journal of the Canadian Academy of Sport Medicine 12 (5):273-278

12. Bogaerts S, De Brito Carvalho C, Scheys L, Desloovere K, D'Hooge J, Maes F, Suetens P, Peers K (2017) Evaluation of tissue displacement and regional strain in the Achilles tendon using quantitative high-frequency ultrasound. PloS one 12 (7):e0181364. doi:10.1371/journal.pone.0181364

13. Bogaerts S, Desmet H, Slagmolen P, Peers K (2016) Strain mapping in the Achilles tendon - A systematic review. Journal of biomechanics 49 (9):1411-1419. doi:10.1016/j.jbiomech.2016.02.057

14. Bojsen-Moller J, Hansen P, Aagaard P, Svantesson U, Kjaer M, Magnusson SP (2004) Differential displacement of the human soleus and medial gastrocnemius aponeuroses

during isometric plantar flexor contractions in vivo. Journal of applied physiology (Bethesda, Md : 1985) 97 (5):1908-1914. doi:10.1152/japplphysiol.00084.2004

15. Bojsen-Moller J, Magnusson SP (2015) Heterogeneous Loading of the Human Achilles Tendon In Vivo. Exercise and sport sciences reviews 43 (4):190-197. doi:10.1249/jes.0000000000000062

16. Booth FW (1982) Effect of limb immobilization on skeletal muscle. Journal of applied physiology: respiratory, environmental and exercise physiology 52 (5):1113-1118. doi:10.1152/jappl.1982.52.5.1113

17. Bring DK, Kreicbergs A, Renstrom PA, Ackermann PW (2007) Physical activity modulates nerve plasticity and stimulates repair after Achilles tendon rupture. Journal of orthopaedic research : official publication of the Orthopaedic Research Society 25 (2):164-172. doi:10.1002/jor.20257

18. Brumann M, Baumbach SF, Mutschler W, Polzer H (2014) Accelerated rehabilitation following Achilles tendon repair after acute rupture - Development of an evidence-based treatment protocol. Injury 45 (11):1782-1790. doi:10.1016/j.injury.2014.06.022

19. Chernak LA, Thelen DG (2012) Tendon motion and strain patterns evaluated with two-dimensional ultrasound elastography. Journal of biomechanics 45 (15):2618-2623. doi:10.1016/j.jbiomech.2012.08.001

20. Chernak Slane L, Thelen DG (2014) The use of 2D ultrasound elastography for measuring tendon motion and strain. Journal of biomechanics 47 (3):750-754. doi:10.1016/j.jbiomech.2013.11.023

21. Chiodo CP, Glazebrook M, Bluman EM, Cohen BE, Femino JE, Giza E, Watters WC, 3rd, Goldberg MJ, Keith M, Haralson RH, 3rd, Turkelson CM, Wies JL, Hitchcock K, Raymond L, Anderson S, Boyer K, Sluka P (2010) American Academy of Orthopaedic Surgeons clinical practice guideline on treatment of Achilles tendon rupture. The Journal of bone and joint surgery American volume 92 (14):2466-2468

22. Cummins EJ, Anson BJ, et al. (1946) The structure of the calcaneal tendon (of Achilles) in relation to orthopedic surgery, with additional observations on the plantaris muscle. Surgery, gynecology & obstetrics 83:107-116

23. Dirks ML, Wall BT, van Loon LJC (2017) Interventional strategies to combat muscle disuse atrophy in humans: focus on neuromuscular electrical stimulation and dietary protein. Journal of applied physiology (Bethesda, Md : 1985):jap009852016. doi:10.1152/japplphysiol.00985.2016

24. Edama M, Kubo M, Onishi H, Takabayashi T, Inai T, Yokoyama E, Hiroshi W, Satoshi N, Kageyama I (2015) The twisted structure of the human Achilles tendon. Scandinavian journal of medicine & science in sports 25 (5):e497-503. doi:10.1111/sms.12342

25. Eliasson P, Andersson T, Aspenberg P (2012) Achilles tendon healing in rats is improved by intermittent mechanical loading during the inflammatory phase. Journal of orthopaedic research : official publication of the Orthopaedic Research Society 30 (2):274-279. doi:10.1002/jor.21511

26. Enwemeka CS (1989) Inflammation, cellularity, and fibrillogenesis in regenerating tendon: implications for tendon rehabilitation. Physical therapy 69 (10):816-825

27. Erdemir A, Hamel AJ, Piazza SJ, Sharkey NA (2003) Fiberoptic measurement of tendon forces is influenced by skin movement artifact. Journal of biomechanics 36 (3):449-455

28. Erdemir A, Piazza SJ, Sharkey NA (2002) Influence of loading rate and cable migration on fiberoptic measurement of tendon force. Journal of biomechanics 35 (6):857-862

29. Finni T, Komi PV, Lepola V (2000) In vivo human triceps surae and quadriceps femoris muscle function in a squat jump and counter movement jump. European journal of applied physiology 83 (4 -5):416-426. doi:10.1007/s004210000289

30. Finni T, Komi PV, Lukkariniemi J (1998) Achilles tendon loading during walking: application of a novel optic fiber technique. European journal of applied physiology and occupational physiology 77 (3):289-291. doi:10.1007/s004210050335

31. Franz JR, Slane LC, Rasske K, Thelen DG (2015) Non-uniform in vivo deformations of the human Achilles tendon during walking. Gait & posture 41 (1):192-197. doi:10.1016/j.gaitpost.2014.10.001

32. Froberg A, Cisse AS, Larsson M, Martensson M, Peolsson M, Movin T, Arndt A (2017) Altered patterns of displacement within the Achilles tendon following surgical repair. Knee surgery, sports traumatology, arthroscopy : official journal of the ESSKA 25 (6):1857-1865. doi:10.1007/s00167-016-4394-5

33. Froberg A, Komi P, Ishikawa M, Movin T, Arndt A (2009) Force in the achilles tendon during walking with ankle foot orthosis. The American journal of sports medicine 37 (6):1200-1207. doi:10.1177/0363546508330126

34. Fukashiro S, Itoh M, Ichinose Y, Kawakami Y, Fukunaga T (1995) Ultrasonography gives directly but noninvasively elastic characteristic of human tendon in vivo. European journal of applied physiology and occupational physiology 71 (6):555-557

35. Fukashiro S, Komi PV, Jarvinen M, Miyashita M (1993) Comparison between the directly measured achilles tendon force and the tendon force calculated from the ankle joint moment during vertical jumps. Clinical biomechanics (Bristol, Avon) 8 (1):25-30. doi:10.1016/s0268-0033(05)80006-3

36. Fukashiro S, Komi PV, Jarvinen M, Miyashita M (1995) In vivo Achilles tendon loading during jumping in humans. European journal of applied physiology and occupational physiology 71 (5):453-458

37. Ginn K, Eastburn G, Lee M (1993) Evaluation of a buckle force transducer for measuring tissue tension. The Australian journal of physiotherapy 39 (1):31-38. doi:10.1016/s0004-9514(14)60467-0

38. Handsfield GG, Slane LC, Screen HRC (2016) Nomenclature of the tendon hierarchy: An overview of inconsistent terminology and a proposed size-based naming scheme with terminology for multi-muscle tendons. Journal of biomechanics 49 (13):3122-3124. doi:10.1016/j.jbiomech.2016.06.028

39. Haraldsson BT, Aagaard P, Qvortrup K, Bojsen-Moller J, Krogsgaard M, Koskinen S, Kjaer M, Magnusson SP (2008) Lateral force transmission between human tendon fascicles. Matrix biology : journal of the International Society for Matrix Biology 27 (2):86-95. doi:10.1016/j.matbio.2007.09.001

40. Helle-Valle T, Crosby J, Edvardsen T, Lyseggen E, Amundsen BH, Smith HJ, Rosen BD, Lima JA, Torp H, Ihlen H, Smiseth OA (2005) New noninvasive method for

assessment of left ventricular rotation: speckle tracking echocardiography. Circulation 112 (20):3149-3156. doi:10.1161/circulationaha.104.531558

41. Holm C, Kjaer M, Eliasson P (2015) Achilles tendon rupture--treatment and complications: a systematic review. Scandinavian journal of medicine & science in sports 25 (1):e1-10. doi:10.1111/sms.12209

42. Huttunen TT, Kannus P, Rolf C, Fellander-Tsai L, Mattila VM (2014) Acute achilles tendon ruptures: incidence of injury and surgery in Sweden between 2001 and 2012. The American journal of sports medicine 42 (10):2419-2423. doi:10.1177/0363546514540599

43. Ishikawa M, Komi PV, Grey MJ, Lepola V, Bruggemann GP (2005) Muscle-tendon interaction and elastic energy usage in human walking. Journal of applied physiology (Bethesda, Md : 1985) 99 (2):603-608. doi:10.1152/japplphysiol.00189.2005

44. Jacobson B (1995) Medicin och teknik. 4 edn. Studentlitteratur, Lund, Sweden

45. Jones MP, Khan RJ, Carey Smith RL (2012) Surgical interventions for treating acute achilles tendon rupture: key findings from a recent cochrane review. The Journal of bone and joint surgery American volume 94 (12):e88. doi:10.2106/jbjs.j.01829

46. Kadel NJ, Segal A, Orendurff M, Shofer J, Sangeorzan B (2004) The efficacy of two methods of ankle immobilization in reducing gastrocnemius, soleus, and peroneal muscle activity during stance phase of gait. Foot & ankle international 25 (6):406-409. doi:10.1177/107110070402500607

47. Kangas J, Pajala A, Ohtonen P, Leppilahti J (2007) Achilles tendon elongation after rupture repair: a randomized comparison of 2 postoperative regimens. The American journal of sports medicine 35 (1):59-64. doi:10.1177/0363546506293255

48. Kangas J, Pajala A, Siira P, Hamalainen M, Leppilahti J (2003) Early functional treatment versus early immobilization in tension of the musculotendinous unit after Achilles rupture repair: a prospective, randomized, clinical study. The Journal of trauma 54 (6):1171-1180; discussion 1180-1171. doi:10.1097/01.ta.0000047945.20863.a2

49. Kannus P, Jozsa L, Natri A, Jarvinen M (1997) Effects of training, immobilization and remobilization on tendons. Scandinavian journal of medicine & science in sports 7 (2):67-71

50. Kearney RS, Lamb SE, Achten J, Parsons NR, Costa ML (2011) In-shoe plantar pressures within ankle-foot orthoses: implications for the management of achilles tendon ruptures. The American journal of sports medicine 39 (12):2679-2685. doi:10.1177/0363546511420809

51. Khan RJ, Fick D, Keogh A, Crawford J, Brammar T, Parker M (2005) Treatment of acute achilles tendon ruptures. A meta-analysis of randomized, controlled trials. The Journal of bone and joint surgery American volume 87 (10):2202-2210. doi:10.2106/jbjs.d.03049

52. Kim YS, Kim JM, Bigliani LU, Kim HJ, Jung HW (2011) In vivo strain analysis of the intact supraspinatus tendon by ultrasound speckles tracking imaging. Journal of orthopaedic research : official publication of the Orthopaedic Research Society 29 (12):1931-1937. doi:10.1002/jor.21470

53. Komi PV (1990) Relevance of in vivo force measurements to human biomechanics. Journal of biomechanics 23 Suppl 1:23-34

54. Komi PV, Belli A, Huttunen V, Bonnefoy R, Geyssant A, Lacour JR (1996) Optic fibre as a transducer of tendomuscular forces. European journal of applied physiology and occupational physiology 72 (3):278-280

55. Komi PV, Fukashiro S, Jarvinen M (1992) Biomechanical loading of Achilles tendon during normal locomotion. Clinics in sports medicine 11 (3):521-531

56. Komi PV, Salonen M, Jarvinen M, Kokko O (1987) In vivo registration of Achilles tendon forces in man. I. Methodological development. International journal of sports medicine 8 Suppl 1:3-8

57. Konrad P (2006) ABC of EMG. vesion 1.4 edn. Noraxon U.S.A Inc., Scottsdale, Arizona, USA

58. Korstanje JW, Selles RW, Stam HJ, Hovius SE, Bosch JG Dedicated ultrasound speckle tracking to study tendon displacement. In: SPIE Proceedings Vol. 7265: Medical Imaging 2009: Ultrasonic Imaging and Signal Processing, Lake Buena Vista, FL, USA, 2009. doi:10.1117/12.811156

59. Korstanje JW, Selles RW, Stam HJ, Hovius SE, Bosch JG (2010) Development and validation of ultrasound speckle tracking to quantify tendon displacement. Journal of biomechanics 43 (7):1373-1379. doi:10.1016/j.jbiomech.2010.01.001

60. Larsson M, Kremer F, Claus P, Kuznetsova T, Brodin LA, D'Hooge J (2011) Ultrasound-based radial and longitudinal strain estimation of the carotid artery: a feasibility study. IEEE transactions on ultrasonics, ferroelectrics, and frequency control 58 (10):2244-2251. doi:10.1109/tuffc.2011.2074

61. Lersch C, Grotsch A, Segesser B, Koebke J, Bruggemann GP, Potthast W (2012) Influence of calcaneus angle and muscle forces on strain distribution in the human Achilles tendon. Clinical biomechanics (Bristol, Avon) 27 (9):955-961. doi:10.1016/j.clinbiomech.2012.07.001

62. Lichtwark GA, Wilson AM (2005) In vivo mechanical properties of the human Achilles tendon during one-legged hopping. The Journal of experimental biology 208 (Pt 24):4715-4725. doi:10.1242/jeb.01950

63. Lichtwark GA, Wilson AM (2006) Interactions between the human gastrocnemius muscle and the Achilles tendon during incline, level and decline locomotion. The Journal of experimental biology 209 (Pt 21):4379-4388. doi:10.1242/jeb.02434

64. Lindgren U, Svensson O (2007) Ortopedi. 3rd edn. Liber AB, Stockholm, Sweden

65. Longo UG, Ronga M, Maffulli N (2018) Achilles Tendinopathy. Sports medicine and arthroscopy review 26 (1):16-30. doi:10.1097/jsa.0000000000000185

66. Maffulli N, Sharma P, Luscombe KL (2004) Achilles tendinopathy: aetiology and management. Journal of the Royal Society of Medicine 97 (10):472-476. doi:10.1258/jrsm.97.10.472

67. Maffulli N, Tallon C, Wong J, Lim KP, Bleakney R (2003) Early weightbearing and ankle mobilization after open repair of acute midsubstance tears of the achilles tendon. The American journal of sports medicine 31 (5):692-700

68. Maganaris CN, Narici MV, Maffulli N (2008) Biomechanics of the Achilles tendon. Disability and rehabilitation 30 (20-22):1542-1547. doi:10.1080/09638280701785494

69. Magnusson SP, Hansen P, Aagaard P, Brond J, Dyhre-Poulsen P, Bojsen-Moller J, Kjaer M (2003) Differential strain patterns of the human gastrocnemius aponeurosis and

free tendon, in vivo. Acta physiologica Scandinavica 177 (2):185-195. doi:10.1046/j.1365-201X.2003.01048.x

70. Metz R, Verleisdonk EJ, van der Heijden GJ, Clevers GJ, Hammacher ER, Verhofstad MH, van der Werken C (2008) Acute Achilles tendon rupture: minimally invasive surgery versus nonoperative treatment with immediate full weightbearing--a randomized controlled trial. The American journal of sports medicine 36 (9):1688-1694. doi:10.1177/0363546508319312

71. Moller M, Kalebo P, Tidebrant G, Movin T, Karlsson J (2002) The ultrasonographic appearance of the ruptured Achilles tendon during healing: a longitudinal evaluation of surgical and nonsurgical treatment, with comparisons to MRI appearance. Knee surgery, sports traumatology, arthroscopy : official journal of the ESSKA 10 (1):49-56. doi:10.1007/s001670100245

72. Moller M, Movin T, Granhed H, Lind K, Faxen E, Karlsson J (2001) Acute rupture of tendon Achillis. A prospective randomised study of comparison between surgical and non-surgical treatment. The Journal of bone and joint surgery British volume 83 (6):843-848

73. Moore KL (1992) Clinically oriented anatomy. 3rd edn. Williams & Wilkins, Baltimore, Maryland, USA

74. Mortensen HM, Skov O, Jensen PE (1999) Early motion of the ankle after operative treatment of a rupture of the Achilles tendon. A prospective, randomized clinical and radiographic study. The Journal of bone and joint surgery American volume 81 (7):983-990

75. Movin T, Ryberg A, McBride DJ, Maffulli N (2005) Acute rupture of the Achilles tendon. Foot and ankle clinics 10 (2):331-356. doi:10.1016/j.fcl.2005.01.003

76. Nilsson-Helander K, Silbernagel KG, Thomee R, Faxen E, Olsson N, Eriksson BI, Karlsson J (2010) Acute achilles tendon rupture: a randomized, controlled study comparing surgical and nonsurgical treatments using validated outcome measures. The American journal of sports medicine 38 (11):2186-2193. doi:10.1177/0363546510376052

77. Nilsson-Helander K, Thomee R, Silbernagel KG, Thomee P, Faxen E, Eriksson BI, Karlsson J (2007) The Achilles tendon Total Rupture Score (ATRS): development and validation. The American journal of sports medicine 35 (3):421-426. doi:10.1177/0363546506294856

78. Olsson N, Silbernagel KG, Eriksson BI, Sansone M, Brorsson A, Nilsson-Helander K, Karlsson J (2013) Stable surgical repair with accelerated rehabilitation versus nonsurgical treatment for acute Achilles tendon ruptures: a randomized controlled study. The American journal of sports medicine 41 (12):2867-2876. doi:10.1177/0363546513503282

79. Orlin MN, McPoil TG (2000) Plantar pressure assessment. Physical therapy 80 (4):399-409

80. Rantanen J, Hurme T, Kalimo H (1999) Calf muscle atrophy and Achilles tendon healing following experimental tendon division and surgery in rats. Comparison of postoperative immobilization of the muscle-tendon complex in relaxed and tensioned positions. Scandinavian journal of medicine & science in sports 9 (1):57-61

81. Razak AH, Zayegh A, Begg RK, Wahab Y (2012) Foot plantar pressure measurement system: a review. Sensors (Basel, Switzerland) 12 (7):9884-9912. doi:10.3390/s120709884

82. Reckefuss N, Butz T, Horstkotte D, Faber L (2011) Evaluation of longitudinal and radial left ventricular function by two-dimensional speckle-tracking echocardiography in a large cohort of normal probands. The international journal of cardiovascular imaging 27 (4):515-526. doi:10.1007/s10554-010-9716-y

83. Roriz P, Carvalho L, Frazao O, Santos JL, Simoes JA (2014) From conventional sensors to fibre optic sensors for strain and force measurements in biomechanics applications: a review. Journal of biomechanics 47 (6):1251-1261. doi:10.1016/j.jbiomech.2014.01.054

84. Rupp S, Tempelhof S, Fritsch E (1995) Ultrasound of the Achilles tendon after surgical repair: morphology and function. The British journal of radiology 68 (809):454-458. doi:10.1259/0007-1285-68-809-454

85. Sandberg OH, Danmark I, Eliasson P, Aspenberg P (2015) Influence of a lower leg brace on traction force in healthy and ruptured Achilles tendons. Muscles, ligaments and tendons journal 5 (2):63-67

86. Schepull T, Aspenberg P (2013) Early controlled tension improves the material properties of healing human achilles tendons after ruptures: a randomized trial. The American journal of sports medicine 41 (11):2550-2557. doi:10.1177/0363546513501785

87. Schepull T, Kvist J, Andersson C, Aspenberg P (2007) Mechanical properties during healing of Achilles tendon ruptures to predict final outcome: a pilot Roentgen stereophotogrammetric analysis in 10 patients. BMC musculoskeletal disorders 8:116. doi:10.1186/1471-2474-8-116

88. Schepull T, Kvist J, Aspenberg P (2012) Early E-modulus of healing Achilles tendons correlates with late function: similar results with or without surgery. Scandinavian journal of medicine & science in sports 22 (1):18-23. doi:10.1111/j.1600-0838.2010.01154.x

89. Silbernagel KG, Steele R, Manal K (2012) Deficits in heel-rise height and achilles tendon elongation occur in patients recovering from an Achilles tendon rupture. The American journal of sports medicine 40 (7):1564-1571. doi:10.1177/0363546512447926

90. Simmonds FA (1957) The diagnosis of the ruptured Achilles tendon. The Practitioner 179 (1069):56-58

91. Sjostrom M, Wahlby L, Fugl-Meyer A (1979) Achilles tendon injury. 3. Structure of rabbit soleus muscles after immobilization at different positions. Acta chirurgica Scandinavica 145 (8):509-521

92. Slagmolen P, Scheys L, D'Hooge J, Suetens P, Peers K, Debeer P, Bellemans J (2012) In regard to: "In vivo strain analysis of the intact supraspinatus tendon by ultrasound speckles tracking imaging" (Journal of Orthopaedic Research, Vol. 29, No. 12, pp. 1931-1937, May 2011). Journal of orthopaedic research : official publication of the Orthopaedic Research Society 30 (12):2054-2056; author reply 2056-2057. doi:10.1002/jor.22174

93. Slane LC, Thelen DG (2014) Non-uniform displacements within the Achilles tendon observed during passive and eccentric loading. Journal of biomechanics 47 (12):2831-2835. doi:10.1016/j.jbiomech.2014.07.032

94. Soroceanu A, Sidhwa F, Aarabi S, Kaufman A, Glazebrook M (2012) Surgical versus nonsurgical treatment of acute Achilles tendon rupture: a meta-analysis of randomized trials. The Journal of bone and joint surgery American volume 94 (23):2136-2143. doi:10.2106/jbjs.k.00917

95. Spooner SK, Smith DK, Kirby KA (2010) In-shoe pressure measurement and foot orthosis research: a giant leap forward or a step too far? Journal of the American Podiatric Medical Association 100 (6):518-529

96. Sun YL, Wei Z, Zhao C, Jay GD, Schmid TM, Amadio PC, An KN (2015) Lubricin in human achilles tendon: The evidence of intratendinous sliding motion and shear force in achilles tendon. Journal of orthopaedic research : official publication of the Orthopaedic Research Society 33 (6):932-937. doi:10.1002/jor.22897

97. Sundström B (1992) Enaxliga problem teknisk balkteori. 6 th edn., Södertälje, Sweden

98. Szaro P, Witkowski G, Smigielski R, Krajewski P, Ciszek B (2009) Fascicles of the adult human Achilles tendon - an anatomical study. Annals of anatomy = Anatomischer Anzeiger : official organ of the Anatomische Gesellschaft 191 (6):586-593. doi:10.1016/j.aanat.2009.07.006

99. Thomopoulos S, Parks WC, Rifkin DB, Derwin KA (2015) Mechanisms of tendon injury and repair. Journal of orthopaedic research : official publication of the Orthopaedic Research Society 33 (6):832-839. doi:10.1002/jor.22806

100. Thompson TC (1962) A test for rupture of the tendo achillis. Acta orthopaedica Scandinavica 32:461-465

101. Twaddle BC, Poon P (2007) Early motion for Achilles tendon ruptures: is surgery important? A randomized, prospective study. The American journal of sports medicine 35 (12):2033-2038. doi:10.1177/0363546507307503

102. Wall BT, Dirks ML, van Loon LJ (2013) Skeletal muscle atrophy during short-term disuse: implications for age-related sarcopenia. Ageing research reviews 12 (4):898-906. doi:10.1016/j.arr.2013.07.003

103. Wang JH, Guo Q, Li B (2012) Tendon biomechanics and mechanobiology--a minireview of basic concepts and recent advancements. Journal of hand therapy : official journal of the American Society of Hand Therapists 25 (2):133-140; quiz 141. doi:10.1016/j.jht.2011.07.004

104. Willits K, Amendola A, Bryant D, Mohtadi NG, Giffin JR, Fowler P, Kean CO, Kirkley A (2010) Operative versus nonoperative treatment of acute Achilles tendon ruptures: a multicenter randomized trial using accelerated functional rehabilitation. The Journal of bone and joint surgery American volume 92 (17):2767-2775. doi:10.2106/jbjs.i.01401

105. Yang G, Crawford RC, Wang JH (2004) Proliferation and collagen production of human patellar tendon fibroblasts in response to cyclic uniaxial stretching in serum-free conditions. Journal of biomechanics 37 (10):1543-1550. doi:10.1016/j.jbiomech.2004.01.005

106. Yoshii Y, Villarraga HR, Henderson J, Zhao C, An KN, Amadio PC (2009) Speckle tracking ultrasound for assessment of the relative motion of flexor tendon and

subsynovial connective tissue in the human carpal tunnel. Ultrasound in medicine & biology 35 (12):1973-1981. doi:10.1016/j.ultrasmedbio.2009.07.004